

Analysis of foils and wings  
operating at low Reynolds numbers

28/02/2013

# Contents

<b>1 Purpose</b>	<b>4</b>
<b>2 Introduction</b>	<b>4</b>
2.1 Code limitations and domain of validity . . . . .	4
2.2 XFLR5's development history . . . . .	4
2.3 Changes introduced in XFLR5 v6 . . . . .	5
2.3.1 Problem size . . . . .	5
2.3.2 Stability and control analysis . . . . .	5
2.3.3 Batch calculations . . . . .	5
2.3.4 3D panel method . . . . .	5
2.3.5 Inertia estimations . . . . .	6
2.4 Code structure . . . . .	6
<b>3 Foil Analysis and Design Modes</b>	<b>7</b>
3.1 General . . . . .	7
3.2 Direct Analysis [Oper] . . . . .	7
3.2.1 Foil object . . . . .	7
3.2.2 Foil Modification . . . . .	7
3.2.3 Analysis/Polar object . . . . .	8
3.2.4 Operating Point (OpPoint) object . . . . .	8
3.2.5 XFoil analysis . . . . .	9
3.2.6 XFoil errors . . . . .	9
3.2.7 Session example Direct Analysis . . . . .	10
3.3 Full Inverse Design [MDES] and Mixed Inverse Design [QDES] . . . . .	11
3.3.1 General . . . . .	11
3.3.2 Session example – Full Inverse Design . . . . .	11
3.3.3 Session example – Mixed Inverse Design . . . . .	11
3.4 Foil Direct Design . . . . .	12
3.4.1 General . . . . .	12
3.4.2 B-splines main features . . . . .	12
3.4.3 Spline Points main features . . . . .	12
3.4.4 Leading and trailing edge . . . . .	12
3.4.5 Output precision . . . . .	12
3.4.6 Digitalization . . . . .	13
<b>4 3D Analysis</b>	<b>13</b>
4.1 Wind and body axis, sign conventions . . . . .	13
4.2 Object Definition . . . . .	14
4.2.1 Wing Definition . . . . .	14
4.2.2 Reference area for aerodynamic coefficients . . . . .	15
4.2.3 Flaps . . . . .	16
4.2.4 Body Design . . . . .	16
4.2.5 Plane Definition . . . . .	17
4.2.6 Inertia estimations . . . . .	18
4.2.7 Mesh . . . . .	20
4.2.8 Symmetry . . . . .	23
4.3 Performance analysis . . . . .	23

---

4.3.1	Theory - General . . . . .	23
4.3.2	Viscous and inviscid calculations . . . . .	24
4.3.3	Lifting Line Theory (LLT) - Non Linear . . . . .	24
4.3.4	Vortex Lattice Method (VLM) - Linear . . . . .	27
4.3.5	3D Panel Method - Linear . . . . .	31
4.3.6	Analysis considerations . . . . .	34
4.3.7	Moments . . . . .	41
4.3.8	Neutral point, Center of pressure, Static Margin . . . . .	42
4.3.9	Efficiency factor . . . . .	42
4.3.10	Wing Operating Points and Wing Polars . . . . .	44
4.3.11	Control analysis – Polar Type 5 and Type 6 . . . . .	45
4.3.12	Interpolation of the XFOIL-generated Polar Mesh . . . . .	45
4.3.13	Streamlines . . . . .	47
4.3.14	Comparison to experimental results . . . . .	47
4.3.15	Comparison to wind tunnel data . . . . .	47
4.3.16	Comparison to Miarex and AVL results . . . . .	50
4.3.17	Session example – Wing Analysis . . . . .	50
4.3.18	Non convergences . . . . .	54
4.4	Stability and control analysis . . . . .	55
4.4.1	Method . . . . .	55
4.4.2	Theory . . . . .	55
4.4.3	Frames of reference . . . . .	55
4.4.4	Coordinates, position, velocity, and rotation vector . . . . .	56
4.4.5	Flight constraints . . . . .	57
4.4.6	State description . . . . .	58
4.4.7	Analysis procedure . . . . .	58
4.4.8	Input . . . . .	59
4.4.9	Output . . . . .	62
4.4.10	Session example – Stability analysis . . . . .	66
<b>5</b>	<b>Code Specifics</b>	<b>68</b>
5.1	XFOIL, AVL and XFLR5 . . . . .	68
5.2	Files and Registry . . . . .	68
5.3	Shortcuts . . . . .	68
5.4	Mouse input . . . . .	68
5.5	Memory . . . . .	69
5.6	Export Options . . . . .	69
5.7	Bugs . . . . .	69
5.8	Open Source Development . . . . .	70
<b>6</b>	<b>Credits</b>	<b>70</b>
<b>7</b>	<b>References</b>	<b>71</b>

---

# 1 Purpose

This document is not intended as a formal help manual, but rather as an aid in using XFLR5. Its purpose is to explain the methods used in the calculations, and to provide assistance for the less intuitive aspects of the software.

## 2 Introduction

### 2.1 Code limitations and domain of validity

Like the original XFOIL, this project has been developed and released in accordance with the principles of the GPL. Among other things, one important point about GPL is that :

This program is distributed in the hope that it will be useful, but WITHOUT ANY WARRANTY; without even the implied warranty of MERCHANTABILITY or FITNESS FOR A PARTICULAR PURPOSE. See the GNU General Public License for more details.

The code has been intended and written exclusively for the design of model sailplanes, for which it gives reasonable and consistent results. The code's use for all other purpose, especially for the design of real size aircraft is strongly disapproved.

### 2.2 XFLR5's development history

The primary purposes for the development of XFLR5 were to provide :

- A user-friendly interface for XFOIL
- A translation of the original FORTRAN source code to the C/C++ language, for all developers who might have a need for it

This was done in accordance with, and in the spirit of, Mark Drela's and Harold Youngren's highly valuable work, which they have been kind enough to provide free of use under the General Public License.

The resulting software is not intended as a professional product, and thus it does not offer any guarantees of robustness, accuracy or product support. It is merely a personal use application, developed as a hobby, and provided under GPL rules for use by all.

For this reason, it should be noted and understood that XFLR5 may not be default-free. Some significant bugs affecting result precision have been reported in the beta releases and corrected.

However, XFLR5 has been thoroughly tested against other software and published experimental results, up to now with some success, and this permits a limited amount of trust in the results it provides.

The algorithms for foil analysis implemented in XFLR5 are exactly the same as those of the original XFOIL code, except for the translation from FORTRAN to C. No changes nor amendments have been made. The translation in itself could have caused new bugs. However, the code has been thoroughly tested against numerous original XFOIL analyses, always with consistent results. It may be found, in some cases, that one of the two programs may not converge where the other will, or that the path to convergence is

---

different from one to the other. This is due to the different manner in which floating point numbers and calculations are processed by the two compilers. Having said this, the converged results are always close, and any differences within the convergence criteria set in the XFOil source code.

Hence, both XFOil and XFLR5 results of airfoil analysis will be referred to herein as "XFOil results".

Wing analysis capabilities have been added in version 2.00. Initially, this was done at the suggestion of Matthieu Scherrer, who has experimented with his Mathlab "Miarex" code the application of the Non-linear Lifting Line Theory (herein referred to as "LLT") to the design of wings operating at low Reynolds numbers.

Later on, the necessity arose to add the Vortex Lattice Method (herein referred to as "VLM") for the design and analysis of wings with geometries not consistent with the limitations of the LLT.

Version v3.00 introduced Katz and Plotkin's recommended VLM method based on quadrilateral rings, and the VLM calculation of planes with elevator and fin.

On March 31<sup>st</sup>, 2007, XFLR5 has become an Open Source Development Project hosted by Sourceforge.net.

Version v4.00 introduces a 3D panel method for wings and planes, including modeling options for fuselages.

Up to this last version, XFLR5 has been developed specifically for Windows, using Microsoft's MFC libraries. This is a limitation of the product, making it non available for Unix, Linux, and MAC systems. It has therefore been decided to re-write the code using the cross-platform Qt4 libraries provided by Nokia. This version has been released as XFLR5 v5. It does not offer any new functionality compared to the original code.

Released in a beta version in September 2010, XFLR5 v6 introduces the stability and control analysis, and a modification of the 3D-panel method for the plane.

## **2.3 Changes introduced in XFLR5 v6**

### **2.3.1 Problem size**

The maximum acceptable size for mesh definitions has been increased from 2000 panels to 5000 panels max.

Since the memory allocation increases as the square power of the problem size, this new version will reserve more memory at the program launch, and may take longer to start on those computer with low RAM.

### **2.3.2 Stability and control analysis**

"Control polars" have been replaced by "stability polars", with evaluation of stability and control derivatives.

### **2.3.3 Batch calculations**

It is now possible to run a batch calculations for a list of airfoils.

### **2.3.4 3D panel method**

The 3D panel method is now processed differently for single wings and for planes.

For the analysis of single wings, the full 3D method is available as in v5, with the wings represented as thick surfaces with uniform doublet and source distribution.

For planes, the full 3D method has been replaced in v6 by a mix formulation of 3D panels for the fuselage, and thin surfaces for the wings.

### **2.3.5 Inertia estimations**

In the inertia evaluation of wings, the mass of each strip is distributed along the strip proportionally to the foils thickness, and is no longer concentrated at the quarter-chord position.

## **2.4 Code structure**

Five different "Applications" have been implemented :

- Two direct design modes which are convenient to compare foils, and to design new foils with the use of B-Splines
- The mixed inverse (QDES) and the full inverse (MDES) foil design routines, virtually unchanged from the original
- The foil direct analysis routines (OPER)
- The wing, plane and body design and analysis

---

## 3 Foil Analysis and Design Modes

### 3.1 General

This part of the code is built around XFoil and its main features, i.e. the design routines, and the direct and inverse analysis (OPER, MDES, GDES, and QDES). Except for the implementation of the Windows interface, no special feature has been added to these modules.

To run and use XFLR5, no special knowledge nor any previous experience of XFoil is necessary, although users accustomed to XFoil should have no difficulty in recognizing the new Windows-style menu options.

Since the analysis engine is very much unchanged from the original, users are advised to refer to the original XFoil help to understand the purpose, operation, and limitations of the foil direct and inverse analysis. Their use in XFLR5 is basically the same, with a limited number of necessary adaptations for the Windows interface.

### 3.2 Direct Analysis [Oper]

#### 3.2.1 Foil object

**Foil Database** Foils are loaded from standard foil files and are stored in a runtime database. Any number of foils may be loaded at any time.

**File format** XFLR5 recognizes only the plain traditional format for foils, i.e. files which contain the foil's name on the first line, followed by the X,Y coordinates, which run from the trailing edge, round the leading edge, back to the trailing edge in either direction:

```
Foil Name
X(1) Y(1)
X(2) Y(2)
. .
. .
X(N) Y(N)
```

All lines containing a # character are ignored.

No special checks are performed on the input geometry. Users are advised to check the file format if the foil is not read properly by XFLR5.

#### 3.2.2 Foil Modification

XFLR5 provides the same options for foil modification as the original XFoil code. These are:

- local and global refinement
- modification of the thickness, camber, max thickness and max camber positions.

The modification of these parameters will cause a new foil to be generated.

Whenever a foil is modified, deleted or overwritten, all its associated results are deleted to ensure consistency.

Experience shows, and XFoil advises, that refinement of the foil's panels, after it has been loaded or modified, is usually a prudent measure to take before any analysis.

### 3.2.3 Analysis/Polar object

Unlike XFOIL, an analysis of a given foil may be performed only after a "polar object" has been defined and associated to this foil. The results of the analysis will automatically be associated and added to the polar object.

Any number of polars may be created and associated to a given foil.

A polar object is defined by:

- its Type
- its Reynolds and Mach numbers
- the laminar to turbulent transition criterion
- the forced trip locations on top and bottom surfaces

By default, the transition number is set to 9, and the trip locations are set at the trailing edge.

In addition to the Type 1, 2 and 3 polars which are unchanged from XFOIL, Type 4 polars have been introduced, showing data for a given angle of attack at variable Re. The purpose is to enable determination of the critical Re value.

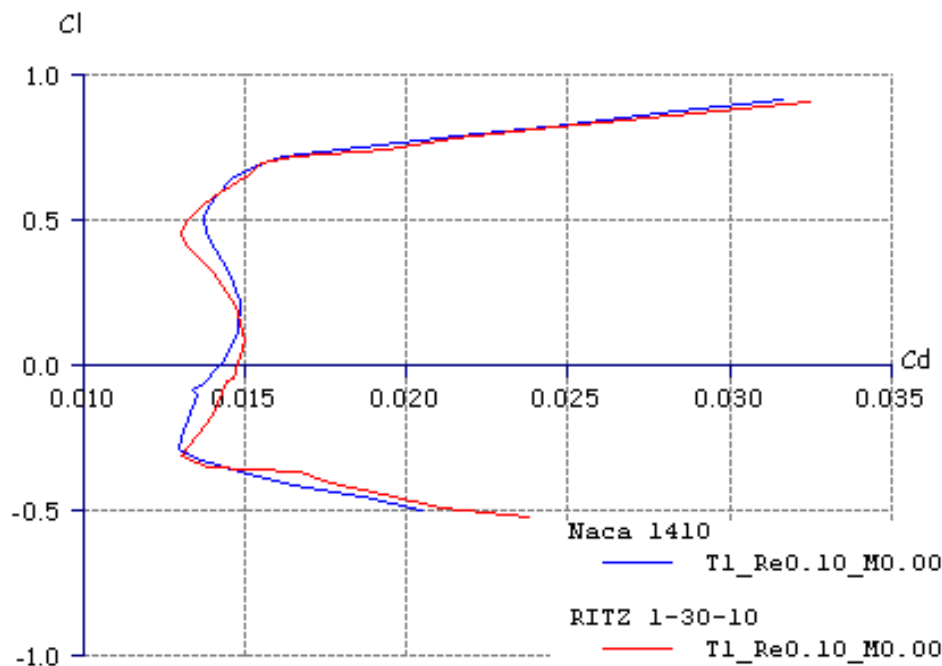


Figure 1: Type 1 foil polars

### 3.2.4 Operating Point (OpPoint) object

An operating point of a given foil is defined by its angle of attack and its Re number. Always associated to a foil and to a Polar object, the OpPoint stores the inviscid and viscous results of the analysis.

Any number of OpPoints may be stored in the runtime database, the only limitation being computer memory. OpPoints may use significant memory resources.



To insure consistency, any modification to the foil or to the polar causes the operating point to be deleted from the database.

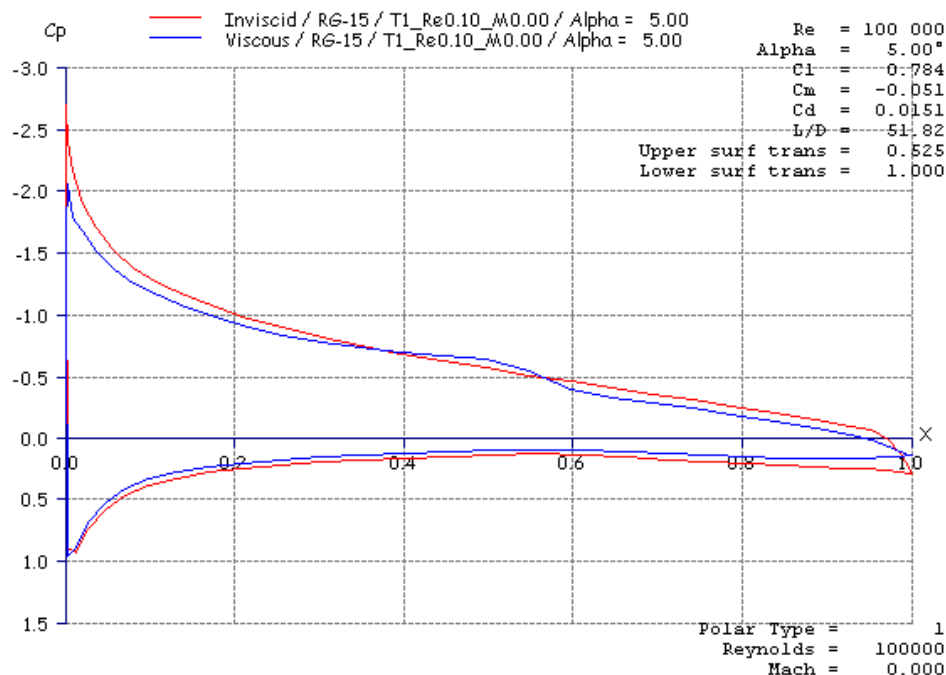


Figure 2:  $C_p$  calculation

### 3.2.5 XFOil analysis

Each time an XFOil direct analysis is performed and the convergence is achieved, an OpPoint is generated and the values of interest are stored in the currently selected polar object. Data is added to the polar, whether the option to store OpPoints has been activated or not.

An XFOil calculation performed at the same angle of attack and  $Re$  as an existing OpPoint causes the latter to be replaced, and the polar data to be updated.

The "Init BL" checkbox is the equivalent of the "Init" menu command in XFOil, i.e., it resets the boundary layer to standard values before an analysis. It is recommended to check the box at the time of the first calculation, and whenever the analysis of an OpPoint is unconverged or is very different from the previous one.

In the case of sequential analysis, the "Init BL" is automatically deactivated after a first converged point has been reached, and is reset after an unconverged calculation.

### 3.2.6 XFOil errors

Given the complexity and difficulty of a viscous analysis, XFOil is remarkably robust and consistent. It may happen however that the following error message is generated during an analysis.

This error message is usually caused by a too coarse paneling of the foil, or a too sharp leading edge. It is possible that in such a case XFOil gets "stuck" and fails at any attempt to perform a new analysis. The menu command "Operating Point/Reset XFOil" can be used to reinitialize all the variables and reset the currently selected foils and polars.

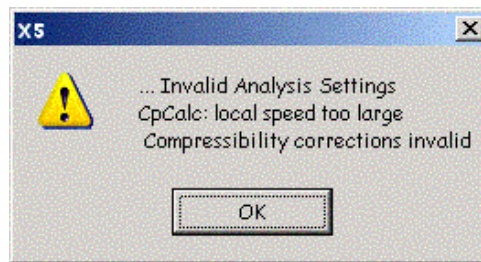


Figure 3: XFoil Error Message

### 3.2.7 Session example Direct Analysis

1. Load a foil from a file
2. (Optional) Use the "Derotate" and "Normalize" commands to respectively align the mean chord with the x-axis and to set its length to 1.
3. (Optional) Use the "Refine Locally" or "Refine Globally" commands to optimize the foil's panels
4. Use the "Define Analysis/Polar" command in the Polar menu, or **F6**, to define an analysis – for instance a Type 1 analysis at  $Re \approx 100000$  and  $Mach = 0.0$
5. Define an angle of attack or a lift coefficient to analyze – for instance  $\alpha = 0^\circ$
6. Click on the "Analyze" button in the right toolbar to launch an analysis
7. If the XFoil analysis has converged, the  $C_p$  distribution will be displayed automatically
8. Check the "Show BL" or "Show Pressure" buttons to visualize either distribution
9. Check the "Sequence" button in the right toolbar
10. Define the min and max angles for the analysis – for instance from  $\alpha = -6^\circ$  to  $\alpha = 10^\circ$
11. Since the new start value is significantly different from the last calculation (i.e.  $\alpha = 0^\circ$ ), check the "Init BLs" button
12. Click on the "Analyze" button
13. Click on the "Animate" button to visualize modifications of the boundary layer or pressure distributions with angle of attack variations
14. Click on the "Polars" command in the View menu, or type **F8**
15. Use the mouse button and wheel to drag and zoom the graphs

---

## 3.3 Full Inverse Design [MDES] and Mixed Inverse Design [QDES]





### 3.3.1 General

Both design modes are unchanged from the original.

Foils generated by the Full Inverse method are defined by 255 coordinate points, which is excessive for subsequent Direct Analysis. A re-paneling of the foil is strongly recommended.

Although foils generated by the Mixed Inverse Method have the same number of panels as the original foil, a re-panel is still advisable.

### 3.3.2 Session example – Full Inverse Design

1. Switch to the Full Inverse Application (Menu command or  +  )
2. Select a foil from the loaded database, or load a foil from a file
3. Click on the "New Spline" button in the right toolbar dialog
4. Select two points either on the upper or lower surface, but not one on each
5. Drag the spline's control points to define a new speed distribution
6. Click on the "Apply" button to register the change
7. Click on the "Execute" button to calculate the new foil geometry
8. Use the mouse buttons and wheel to drag and zoom the graph and the foil
9. Repeat the process until the desired geometry is reached
10. To store the modified foil, click on the arrow in the top toolbar, or select "Store foil in the database" in the Foil menu
11. Switch to the Direct Analysis Application (Menu or  +  )
12. Use "Refine globally" in the Design menu to generate a coarser panel
13. Proceed with the direct analysis

### 3.3.3 Session example – Mixed Inverse Design

Steps 1 to 6 are identical to the Full Inverse design method

7. Click on the "Mark for Modification" button to define which part of the foil is to be modified
8. Click on the "Execute" button to calculate the new foil geometry
9. Check for convergence in the text window  
In the case of non-convergence, it is possible either to resume iterations by clicking again the "Execute" button, or to export the modified geometry as it is

Finish as with the Full Inverse design method.

## 3.4 Foil Direct Design

### 3.4.1 General

A crude design module has been included in XFLR5, which allows the design of Foils either from B-Splines or from "Splined Points". The former gives smoother surfaces, the latter authorizes greater control over the geometry.

This design mode however is not the best way to design foils, and the other possibilities derived from XFOil are far more adapted and recommended i.e. :

- modification of a foil's thickness and camber
- interpolation of foils
- inverse methods

This foil design mode, however, may be useful to overlay different foils and compare their geometries.

An option has been added in v6 to load a background image, with the idea of digitalizing existing foils.

### 3.4.2 B-splines main features

Upper and lower surfaces are each determined by a separate and single B-Spline. Spline degree can be set between 2 and 5.

### 3.4.3 Spline Points main features

Upper and lower surfaces are each determined by a set of control points

Control points are linked by 3rd degree B-Splines

Two intermediate control points are added to the link splines, at 1/3 and 2/3 respectively of the separation of the two control points. These two points are added automatically and are not visible, nor can they be modified.

The slope at each visible control point is determined by the line passing through the immediately previous and next control points.

### 3.4.4 Leading and trailing edge

For both methods, the slope at the leading edge is vertical and may not be changed. In the case of a design from B-Splines, this is done by forcing the second control point to remain on the vertical axis.

In the case of "Splined Points" the slope at the trailing edge is determined by the position of two supplementary rear points, one for each surface.

### 3.4.5 Output precision

The maximum number of output points on each surface is 150. This is consistent with the sizing of the XFOil arrays, and with the precision required for the application, although the increase of computing power and memory capacity of modern computers could allow for more points. Typically, XFOil requires at least 50 points on each side to perform an adequate analysis.

---

In both cases, it is prudent to "re-panel" the foil in the main menu, to improve the convergence of the XFOil analysis and its precision. This can be done with the equivalent of XFOil's "PANE" and "CADD" commands.

Upon exit from the design module, the user is asked whether to export or not the foil to the analysis module.

### 3.4.6 Digitalization

An option has been added in v6.02 to load a background image. The purpose is to enable digitalization of existing foil images using splines.

After digitalization, the splines should be stored as a foil in the database, and the foil ought to be normalized, de-rotated and re-paneled.

## 4 3D Analysis

### 4.1 Wind and body axis, sign conventions

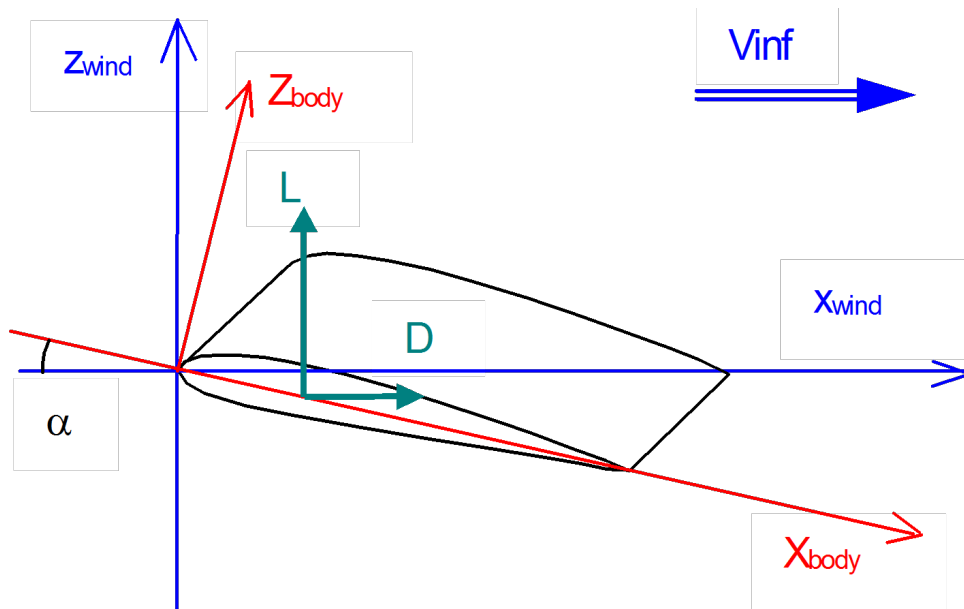


Figure 4: Wind and Body axis

The lift and drag coefficients are given in wind axis.

#### Notes

- Up to v3.21, calculations have been performed using a small angles approximation, which means that the wind and body axis were the same.
- Sign Conventions for moments – Quote from Wikipedia, Flight Dynamics :

The most common aeronautical convention defines the roll as acting about the longitudinal axis, positive with the starboard wing down. The yaw is about the vertical body axis, positive with the nose to starboard. Pitch is about an axis perpendicular to the longitudinal plane of symmetry, positive nose up.

This is illustrated in the Figure 5.

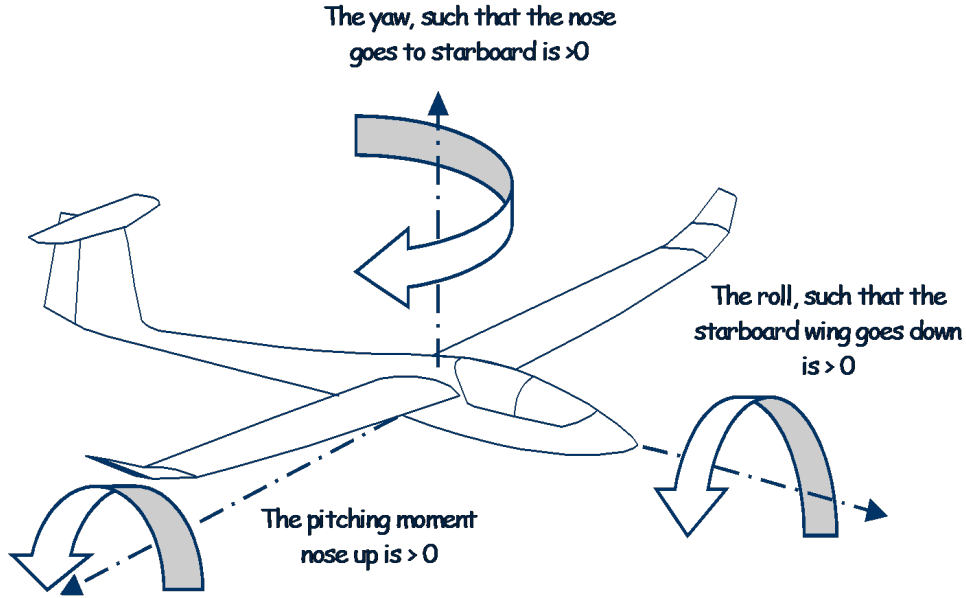


Figure 5: Moment sign convention

## 4.2 Object Definition

### 4.2.1 Wing Definition

The wing is defined as a set of panels. Each panel is defined by :

- its length  $l_i$ ,
- the root and tip chords  $c_i$  and  $c_{i+1}$ ,
- the leading edge offset at root and tip chords  $h_i$  and  $h_{i+1}$ ,
- the dihedral angle  $\delta_i$ ,
- the mesh for VLM analysis.

The spanwise length of a panel should be at least equal to the minimum length of the VLM elements on other panels. Divisions by zero or non-physical results could result from panels of insufficient length.

Twist (washout) is processed in LLT as a modification of the angle of attack.

In VLM, the twist is processed as a modification of the wing, with the rotation center located at the quarter chord point.

Up to v3.04, the twist has been applied as a rotation of the sections with respect to the absolute y axis. From v 3.05 onwards, the sections are rotated with respect to the panel's quarter chord, i.e., after the panel has been rotated by the dihedral angle. The results are impacted for wings with panels well off the x-y plane.

The 'span' of the wing is defined as

$$S = 2 \times \sum l_i$$

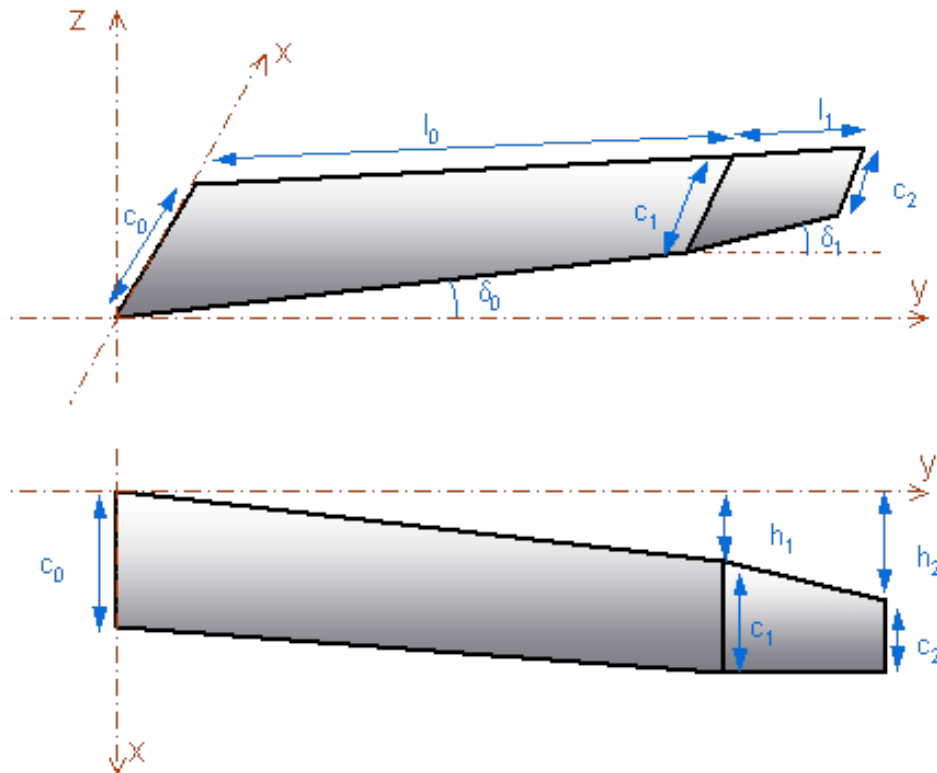


Figure 6: Wing Definition

For ease of interpretation, the wing is shown developed on a horizontal planform, both in the wing design dialog box and in the 2D view. Only the 3D view gives a realistic representation of the geometry.

A wing may be asymmetric if the foils are different on each side. This option is meant to provide some capability to evaluate the influence of flaps, but should be used with caution. It has been tested neither against experimental nor theoretical results.

#### 4.2.2 Reference area for aerodynamic coefficients

The reference area for all wing and plane aerodynamic coefficients is the main wing's area. In the case of a bi-plane, the reference area is also the main wing's area.

There reference lengths for moment coefficients are defined in §4.3.7.

Notes :

- Up to v.4.15, the reference area and the reference span have been defined as the planform's area and span. With this convention, the winglets' contribution are counted in the area and in the span. This is not necessarily the best choice, since it is usually convenient to compare performance coefficients of a wing with and without winglets, but with a constant reference area.
- Starting in v4.16, the default option is to use the planform area and span projected on the xy plane. With this definition, the contribution of the winglets to span and area is zero. For convenience, it is still possible to choose either reference area; the option can be set in the dialog box for analysis definition.

### 4.2.3 Flaps

From version v3.16 onwards, the automatic mesh methods takes into account the breaks at the flap position, if both foils at each end of the wing panel are defined with a flap. The recommended way to create a flap is to define two foils at the same spanwise position, the first with a flap break, the other without. The code will ignore the zero-length panel.

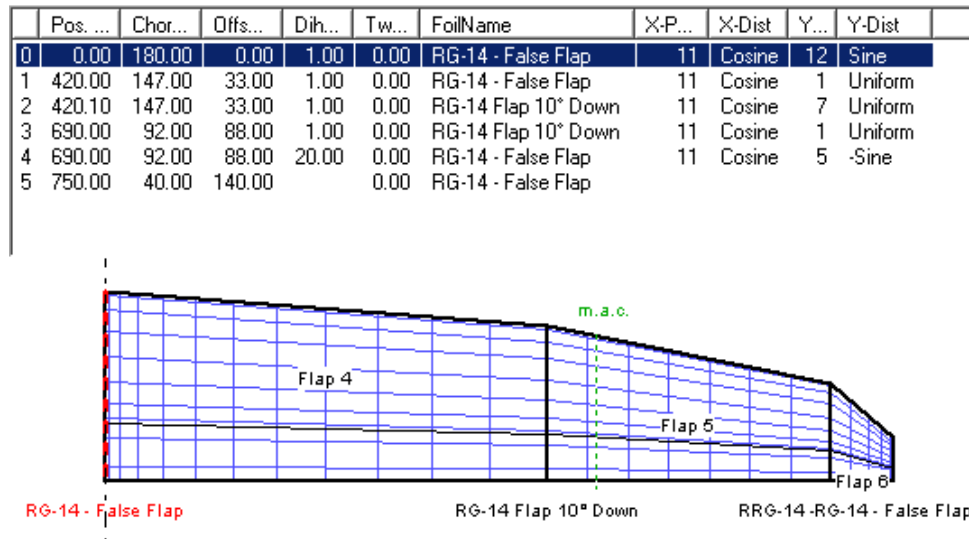


Figure 7: Flap Definition

Triangular flaps, defined by a plain foil at one side of the panel and by a flap break at the other side, are not recognized.

The flaps are counted as one for each wing side, e.g. ailerons are counted as two flaps. This is necessary to calculate separately hinge moments for asymmetrical wings.

### 4.2.4 Body Design

The modeling of the body is natural in a 3D panel method, but isn't either without difficulties.

**Modeling options** Two options are provided, for two different purposes :

1. Representation by flat panels : this is the "Analysis" purpose.  
Given an existing body, the idea is to digitalize its geometry and input it in XFLR5. The resulting geometry will not be smooth, but it is usually enough for prediction purposes
2. Representation by B-Splines : this is the "Design" purpose.  
The idea is to define and optimize a body geometry to achieve some targeted aerodynamic (or cosmetic) performance. The body points can then be exported to a text file for further use.

**Import/export of body data** To facilitate the edition process, the control points can be edited in a text file and imported in XFLR5, rather than being defined directly in XFLR5.



---

An example of the format of the input file can be obtained by exporting any existing body definition.

A typical format is :

```
Body_Name
...
FRAME
x_1 y_2 z_1
...
x_n y_n z_n

OFFSET
X_o Y_o Z_o

BODYTYPE
1 or 2
```

Notes :

- The keywords should be preceded by the character '#'.
- n is the number of side point defining the frame. This number must be the same for all frame. If the frames are defined with different numbers of points, the frame last defined will set the number of points.
- The frames are sorted by x positions
- The points in the frame should be defined in clockwise order, on the body's left side, when looking at the body from the front; this is the view which is displayed in the right panel in the body design module.
- All points in a frame should have the same axial position
- The x position of a frame is defined by the first point

#### 4.2.5 Plane Definition

A plane consists in a main wing, and optionally of a secondary wing, an elevator, one or two fins, and a body.

The body may be described either by cross-sections located at different streamwise locations or by NURBS surfaces.

**Surface assemblies** The main difficulty with the construction of a 3D plane model is to connect the wing, elevator, fin and body together. Without the help of a CAD system, it has been difficult to implement a versatile and robust algorithm, mainly because of the number of configurations to consider. For instance, the elevator may or may not intersect the body, it may or may not intersect the fin, it may intersect the body only on its bottom or upper surface, etc.

The only surface verification implemented in V4.00 is a trim of the wings, elevator and fin to the body's surface, and even then, the algorithm may not be robust for all configurations.

What's more, even if the wings, elevator and fin are trimmed to the fuselage surface, the body's panels are not adapted to follow their contour. This implies that some of the body's panels will be located inside the volume, which is not consistent with the panel theory.

**Tip Patches** The Panel Theory requires that the volume on which the analysis is performed is completely closed by the surfaces which support the panels. In other words, a body or a wing cannot have an open end, in which case a numerical error will occur. To try to close the volumes, the code will automatically create tip patches in the following cases :

- Left tip of the left wing, and right tip of the right wing
- Top and bottom tips of fins

It will not create patches in the following cases :

- Gap at the center of the wing, i.e. if the first chord is located at a positive span position
- Junction of the wing and fuselage

Note : the influence of these modeling errors on the results is unknown.

#### 4.2.6 Inertia estimations

A calculation form is available to provide an approximate evaluation for the CoG position and for the inertia tensor associated to the geometry. The evaluation should not be understood as anything else than a rough order of magnitude.

The inertia is evaluated in the default coordinate system, i.e. with respect to the CoG. The tensor in other systems can be computed by the appropriate tensor transformations. The evaluation is based on the following assumptions.

- For the body, the mass is distributed uniformly in the external surface, and this surface is assumed to have a uniform thickness. The body is divided in  $N_b$  elementary sections along the x-axis. The weight is concentrated at the center of the cross section. This is illustrated in Figure 44.
- For the wings, the mass is assumed to be distributed uniformly in the wing volume along the span.  
In XFLR5 v5, it has been modeled as point masses concentrated at the quarter-chord point of distributed sections along the span.  
In XFLR5 v6, it is modeled as point masses distributed both in the span and chord directions, as illustrated in Figure 45.
- The mass distribution is independent of the wing's mesh used for aerodynamic calculations
- Parts such as actuators, battery, lead, or receiver should be modeled separately as point masses.

---

Notes :

- At this stage of the code development, the results are not used at any point in the performance calculations. The inertia evaluations are provided as a convenience for external stability analysis to be performed with codes such as AVL.
- The mass defined for wings and bodies is not the one used for Type 2 calculations. The mass for type 2 is defined with the Analysis/Polar.

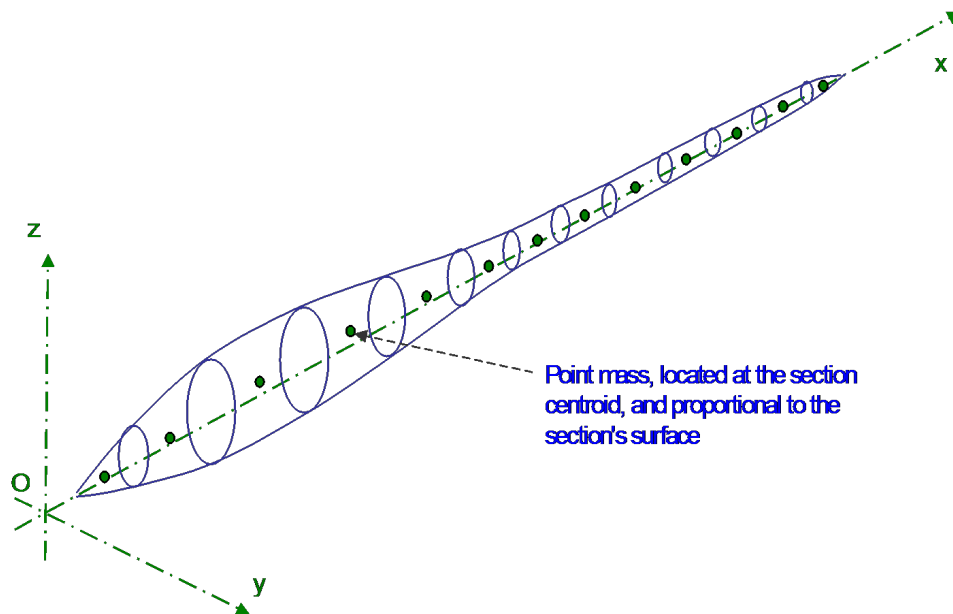


Figure 8: Mass representation for the body

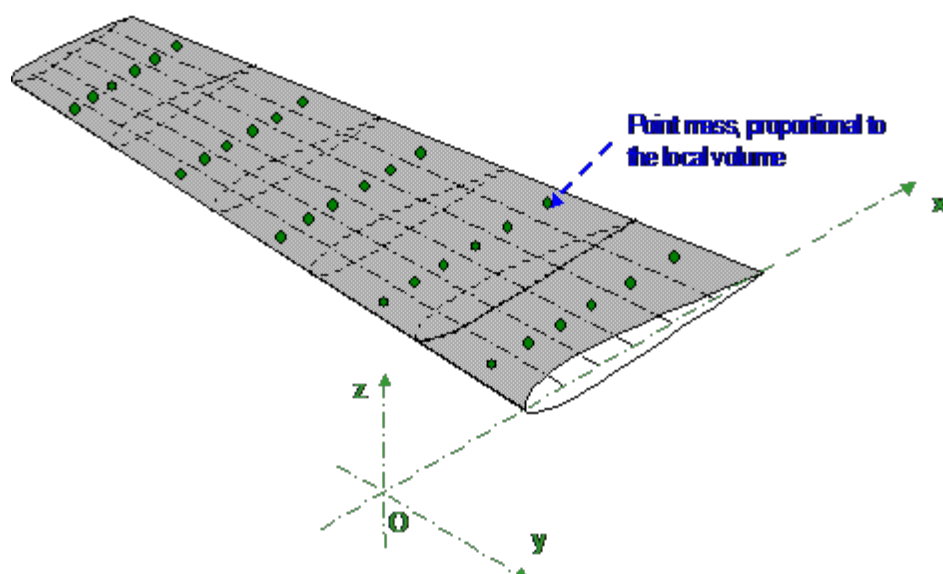


Figure 9: Mass representation for the wing

#### 4.2.7 Mesh

The wing is "meshed" into a number of panels distributed over the span and the chord of the planform, and a vortex or a doublet and source is associated to each panel.

- The analysis may be of the VLM type and is performed on the mean camber line
- The analysis may be of the 3D-panel type in which case the wing is modeled as a thick surface

It is recommended to choose a panel distribution which is consistent with the wing's geometry, i.e. the density of the mesh needs to be increased at geometrical breakpoints and at the root and tip of the wings. A cosine type distribution is recommended in the chordwise direction to provide increased density at the leading and trailing edges.

There is a lower limit size for the panels below which the calculation becomes unstable, or which leads to non-physical results. This can typically occur with "sine" spanwise distributions of panels. Ideally, the precision of the calculation increases with the mesh's refinement, but so do the calculation times. It is fairly simple to experiment to determine what is the best compromise for a given design objective.

Numerical instability may also occur in 3D Panel analysis if a panel's lengths in the streamwise and chordwise directions are too different. The panel's aspect ratio should be kept low.

It is possible to exclude from the calculations the wing panels with a spanwise length less than a minimum value. This can be set in the advanced settings dialog box. If the minimum length is set to zero, then all wing panels with length less than 1/1000 of the span will be excluded. This is meant to avoid numerical errors linked to small mesh elements.

Panel Methods :

1. The current implementation uses flat 1<sup>st</sup> order panels.  
Ideally, these kind of panels need to have their four corners in the same plane, which is not possible for twisted geometries. However, this is not seen as a major issue for the low washout angles used for model sailplane wings.
2. The surface velocity is the gradient of the doublet strengths between adjacent panels as described in [4]. It is therefore recommended to have the same number of chordwise panels along the span, and the same type of distribution, either uniform or sine.  
Ideally, the panels should share the same edges and corner nodes. In the case of a flap, the 'trick' to connect properly the panels is to define a foil with a false flap set at 0° flap angle, as is illustrated in Figure 10.

**Panel arrangement - VLM analysis** Special care must be taken in the disposition of VLM panels to avoid having a control point of the tail's surface close to the trailing leg of one of the wing's horseshoe vortex. This would lead to a division by zero, and inconsistent results.

One method to avoid this issue is to have the wing's panels aligned with those of the elevator.

For the same reason, it is a good idea, though not compulsory, to position fins in the planes of the wing's panel junctions.

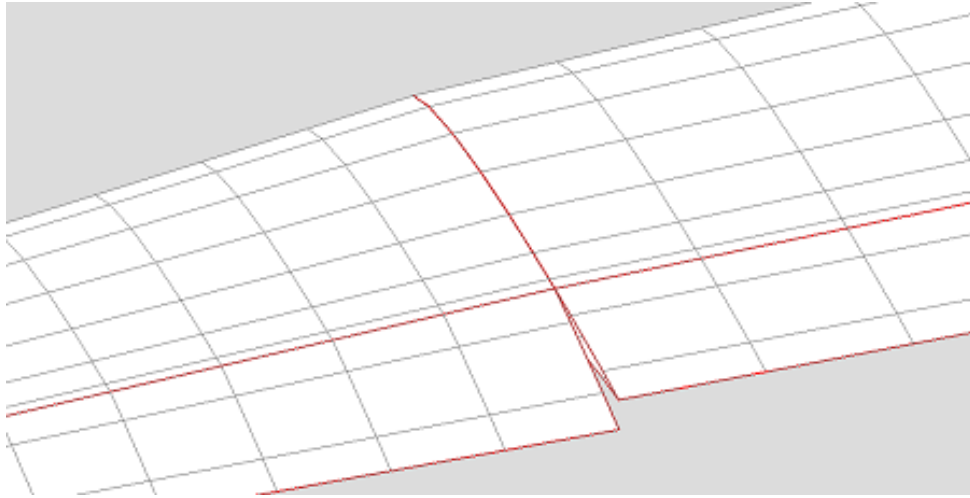


Figure 10: Mesh disposition for a flap

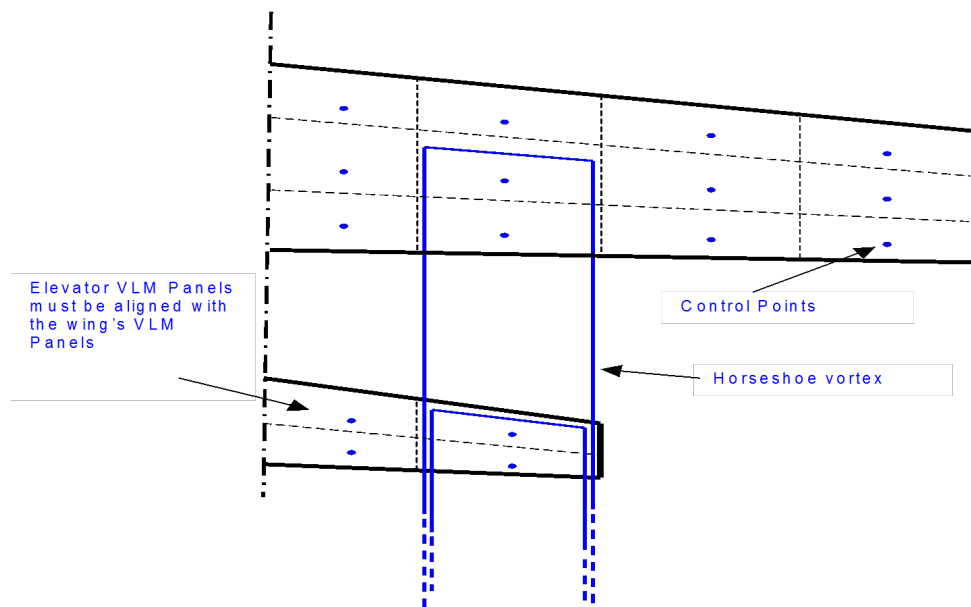


Figure 11: VLM Panel arrangement for a plane

## Panel arrangement - 3D panel analysis

**Chordwise panels** The  $C_p$  distribution is calculated as the derivative of the doublet strength along the panel chordwise and spanwise strips. To achieve this, it is required that each wing has a uniform number of chordwise mesh panels along the span. It is also recommended that the chordwise panel distribution be the same from one wing panel to the next, i.e. cosine distribution for each wing panel. This is necessary to connect adequately the mesh panels at junctions between wing panels.

Mesh panels located in flaps are not connected to the adjacent wing panel. The remaining connections at the junction are performed using the method described in [4].

**Wake Panels** In the VLM method, the wake is represented by the trailing legs of the horseshoe vortices.

In the 3D-panel method, the wake is modeled as a series of flat panels which extend 'far behind' the wing.

The idea is that each of the wing's chordwise strip sheds a column of wake panels. The doublet strength of each panel in this wake strip is the difference of the doublet strength of the top and bottom panels of the wing's strip. This is a consequence of the fact that the wake cannot sustain load. In addition, being a thin surface, the wake panels have a zero source strength.

The wake strips are modeled as a column of thin panels. In the simplest form, these wake panels are straight aligned behind the wing panels, as illustrated in Figure 12.

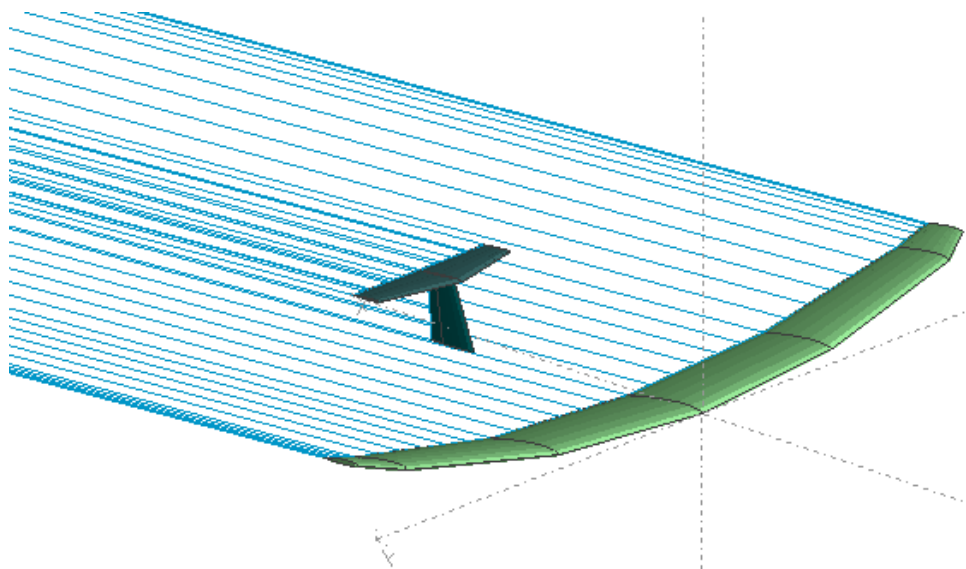


Figure 12: Straight wake

In a more refined and realistic implementation, the wake is aligned with the streamlines which trail behind the wing. Since the doublet distribution on the wing, and the streamlines, in turn depend on the wake shape, an iteration process is required to reach a converged state. This is usually referred to as the "wake relaxation process".

The wake relaxation is a difficult process which can easily diverge. Numerical experiments in XFLR5 have shown that the wake panels are highly warped at the wing tips where the wake strongly rolls up on itself. The convergence requires close control by the

---

user of key parameters such as number of wake panels, length of wake panels or time steps. For these reasons, the wake roll-up process has been disabled.

The wake panels are therefore defined as flat panels which extend behind the wings trailing edges. Their length is  $100 \times \text{MAC}$ . At this distance, the influence of the plane's panels is negligible.

A difficulty arises whenever one of the straight wake panels shed by a surface such as the wing, goes through another surface such as the elevator, as illustrated in Figure 13a. This will lead to unrealistic, non physical results.

In such a situation, it is necessary to modify slightly the geometry to avoid the interference Figure 13b.

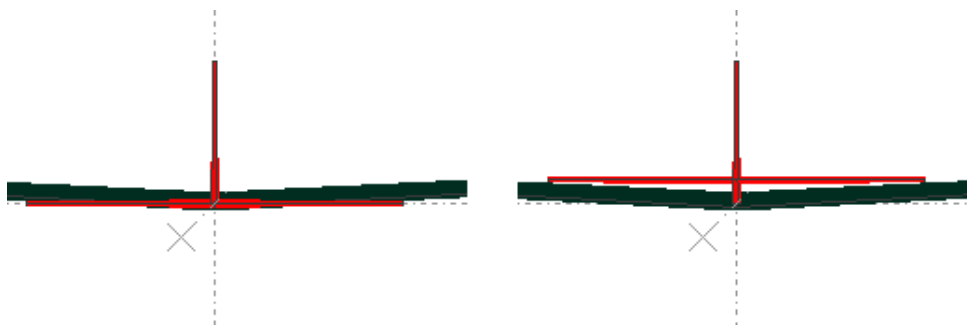


Figure 13: a & b : Wake Interference between wing and elevator

#### 4.2.8 Symmetry

A symmetric calculation reduces the matrix's size by approximately half (exception is the fin), and reduces the matrix inversion operations by a factor 4. The code detects automatically whether the problem is symmetric or not. It is considered to be symmetric in the following cases :

- The wing is symmetric in a Wing-only calculation
- The plane is symmetric without a fin, or with a double fin

The problem is asymmetric otherwise :

- if any of the wings, elevator or fin is asymmetric
- if the plane has a fin

### 4.3 Performance analysis

#### 4.3.1 Theory - General

XFOIL provides unique insight in the behavior of airfoils, but is a 2D analysis, hence the results are those of a wing of infinite aspect ratio and which is defined with a single airfoil. The influence that the aspect ratio alone may have on the wing's polars, let alone the sweep or the dihedral, justifies the need for a more sophisticated wing analysis.

The wing may be computed by either one of three methods, each having its own advantages, and all having some usage restrictions.

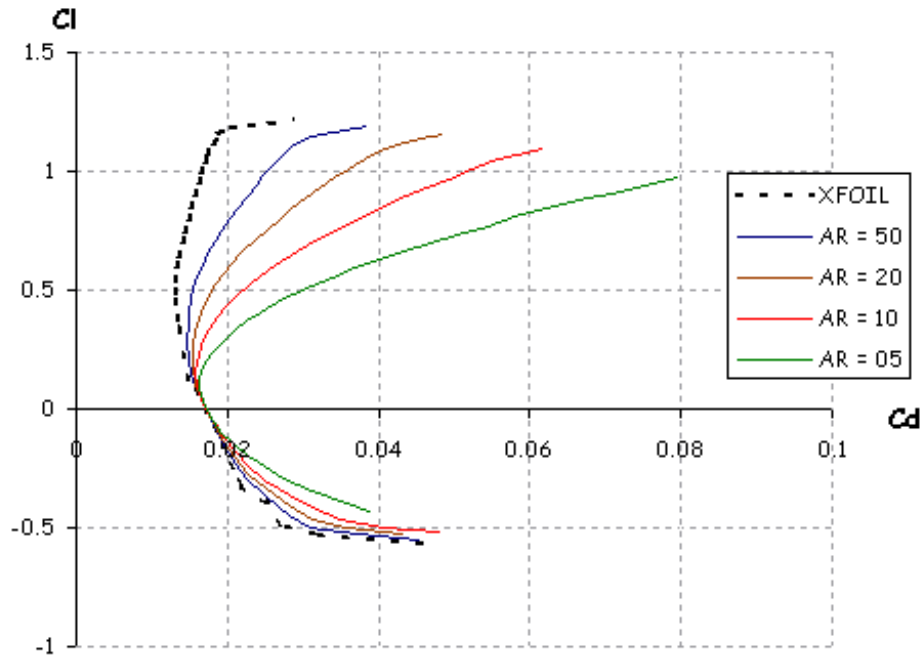


Figure 14: Influence of Aspect Ratio - LLT Calculation NACA 3412 Airfoil - Taper Ratio = 1 - Sweep =  $0^\circ$

The first is a Lifting Line method, derived from Prandtl's wing theory. The second is a Vortex Lattice method. The third is a 3D panel method.

The originality of the implementations is their coupling with XFoil calculation results to estimate the viscous drag associated with the wing, although this is done in a different manner depending on the method.

#### 4.3.2 Viscous and inviscid calculations

In VLM and panel methods, an inviscid analysis/polar may be defined, in which case there is no need to define a polar mesh for the foils. The viscous characteristics will be set to zero.

The LLT is necessarily viscous.

#### 4.3.3 Lifting Line Theory (LLT) - Non Linear

**General** The 'classic' LLT is linear, i.e. the relation  $C_l = f(\alpha)$  is linear, and viscous effects are not taken into account. In the present application, a non-linear LLT has been implemented based on the NACA technical note 1269 [1].

Quote from Technical Note 1269 :

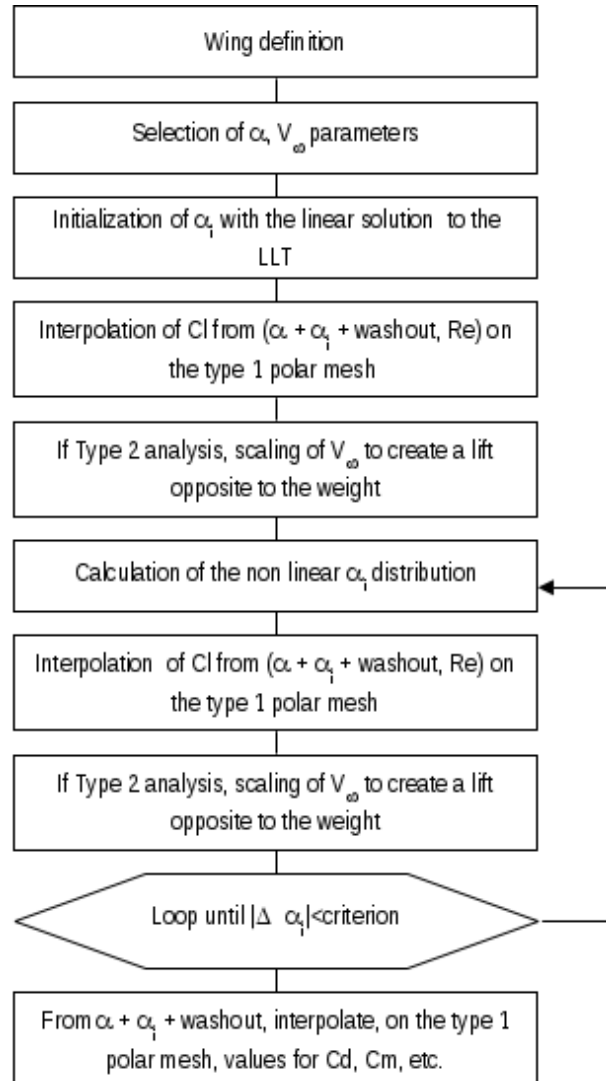
The hypothesis upon which the theory is based is that a lifting wing can be replaced by a lifting line and that the incremental vortices shed along the span trail behind the wing in straight lines in the direction of the freestream velocity. The strength of these trailing vortices is proportional to the rate of change of the lift along the span. The trailing vortices induce a velocity normal to the direction of the free-stream velocity. The effective angle of



attack of each section of the wing is therefore different from the geometric angle of attack by the amount of the angle (called the induced angle of attack) whose tangent is the ratio of the value of the induced velocity to the value of the freestream velocity. The effective angle of attack is thus related to the lift distribution through the induced angle of attack. In addition, the effective angle of attack is related to the section lift coefficient according to two-dimensional data for the airfoil sections incorporated to the wing. Both relationships must be simultaneously satisfied in the calculation of the lift distribution of the wing.

If the section lift curves are linear, these relationships may be expressed by a single equation which can be solved analytically. In general however, the section lift curves are not linear, particularly at high angles of attack, and analytical solutions are not feasible. The method of calculating the spanwise lift distribution using non-linear section lift data thus becomes one of making successive approximations of the lift distribution until one is found that simultaneously satisfies the aforementioned relationships.

The present implementation, the non linear lift behavior is interpolated on pre-generated meshes of XFoil Type 1 polars and the non-linearity is solved by an iteration loop :



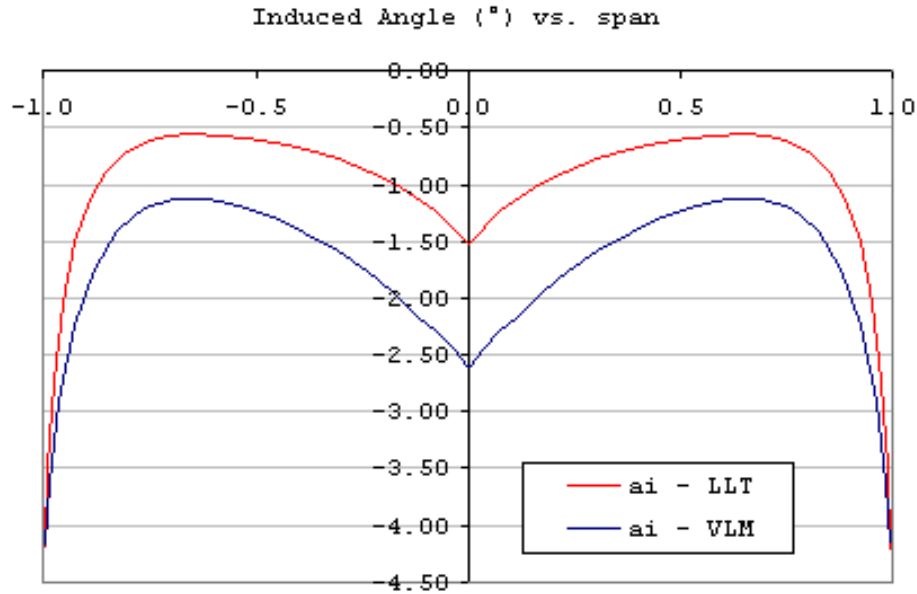


Figure 15: Induced Angle – Bi-Airfoil NACA3412-NACA1410 – AR = 14.8 – TR = 2.0 –  $Alfa = 5^\circ$  –  $V = 16.7\text{m/s}$

**Limitations of the LLT** It is important to note that the lifting line theory has two main limitations. Quote from Technical Note 1269 [1] :

The calculations are subject to the limitations of lifting line theory and should not be expected to give accurate results for wings of low aspect ratio and large amounts of sweep

In addition, the wing's planform is expected to lie essentially in the X-Y plane, i.e. with low dihedral.

**Precautions with the LLT** As it turns out, the convergence of the non-linear LLT is not a robust process, and requires careful use of a relaxation factor. This factor should always be greater than 1. A value of 20 is usually a good start, and may be increased as necessary for convergence.

Usually wings with low aspect ratio require high relaxation value.

The number of stations across the wing span should be chosen around 20, but may be increased up to 40. Greater numbers do not improve the precision of the analysis, but tend to seriously hinder the convergence. The relaxation factor should be increased with higher numbers of span stations.

**2D vs. 3D** The LLT assumes implicitly that all the surfaces lie essentially in the X-Y plane.

The only use for the sweep and the dihedral in this implementation of the LLT is for the calculation of the pitching moment coefficient  $C_m$ .

Sweep and dihedral are not used in the calculation of the lift distribution.

---

**Viscous and inviscid calculations** There is no option available to perform a non-viscous LLT calculation. The reason behind is that the linear theory requires that a zero-lift angle be defined for each airfoil, and that there is no convenient manner to define this  $\alpha_0$  value which depends on the Reynolds number.

**Lift center of pressure** Up to v3.11, the position of the lift center at each span location has been calculated using the usual approximation for thin airfoils, i.e. :

$$X_{CP} = 0.25 - \frac{C_{m0}}{C_l}$$

From v3.12 onwards, the wing's Center of Pressure's x-position is calculated by interpolation of the center of pressure's position on the foil's polar mesh.

For foil polar meshes generated prior to v3.05, the foil's center of pressure was not stored, hence the formula above is used to calculate the wing's center of pressure.

**Downwash** The downwash is defined at each span station as

$$V_i = V_\infty \sin(\alpha_i)$$

For convenience, it is represented at the wing's trailing edge in 3D views.

#### 4.3.4 Vortex Lattice Method (VLM) - Linear

**VLM General principles** A VLM method has been implemented as an alternative, for the analysis of those wing geometries which fall outside the limitations of the LLT.

The main differences from the LLT are:

- The calculation of the lift distribution, the induced angles and the induced drag is inviscid and linear i.e. it is independent of the wing's speed and of the air's viscous characteristics.
- The method is applicable to any usual wing geometry, including those with sweep, low aspect ratio or high dihedral, including winglets.

The principle of a VLM is to model the perturbation generated by the wing by a sum of vortices distributed over the wing's planform. The strength of each vortex is calculated to meet the appropriate boundary conditions (BC), i.e. non penetration conditions on the surface of the panels.

A comprehensive description of the principles of VLM analysis is well outside the scope of this document. Only the main features necessary to a sound use of the code are detailed hereafter.

The resolution of the VLM problem requires the inversion of a square matrix of the size of the number of panels. This inversion is performed by Gauss' partial pivot method. The problem's size may be significantly reduced by considerations of symmetry, detailed in §4.2.8.

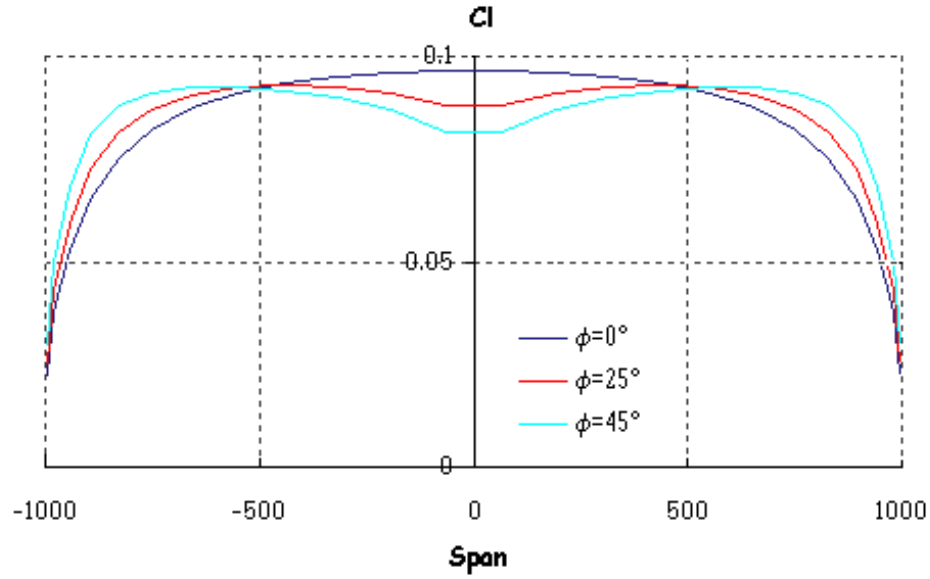


Figure 16: Influence of Sweep for a given CL - AR=10 - TR=1 - Symmetric Airfoil

**Lift force and lift coefficient** The force acting over each panel is the vector cross product

$$F = \rho V \times \Gamma$$

$\Gamma$  being the vortex strength x its length

$\rho$  is the fluid density

$V$  is the freestream speed

Which implies that the force is normal to each panel.

The lift coefficient is defined as

$$C_L = \frac{1}{\rho S V^2} \sum_{panels} F_{wz}$$

$S$  is the sum of the panels' area, i.e. the planform's area

$F_{wz}$  is the projection on the vertical wind axis

This formula is applicable both to a chordwise strip and to the wing's total surface.

The pitching moments and center of pressure position at each span location are calculated by summation of the lift force over the panels.

## Limitations of the VLM

1. The VLM algorithms first computes the lift coefficient  $C_L$  and the other values which may be calculated by integration of the surface forces, i.e. the moment coefficients and the center of pressure's position. The viscous variables (viscous  $C_d$ , transitions, etc) are interpolated from the value of  $C_L$  on the previously XFOIL-generated polars. This obviously raises an issue for high and low  $C_L$ , where the Type 1 polar curve may be interpolated either before or after the stall angle. VLM results should therefore not be considered around angle of attack values close to stall angles.

2. In the current formulation, the VLM makes the assumptions of the small angle of attack. As a main consequence, the trailing vortices are not aligned with the freestream velocity. This means that the influence matrix will be independent of the a.o.a.

To explore this limitation, it is possible to experiment a calculation of the tilted geometry, as explained in §4.3.6. The results tend to show that the assumption of small angles of attack is acceptable.

**VLM alternative method** In the "classic" VLM method, a horseshoe vortex is positioned at the panel quarter chord and the non-penetration condition is set at the three-quarter chord point.

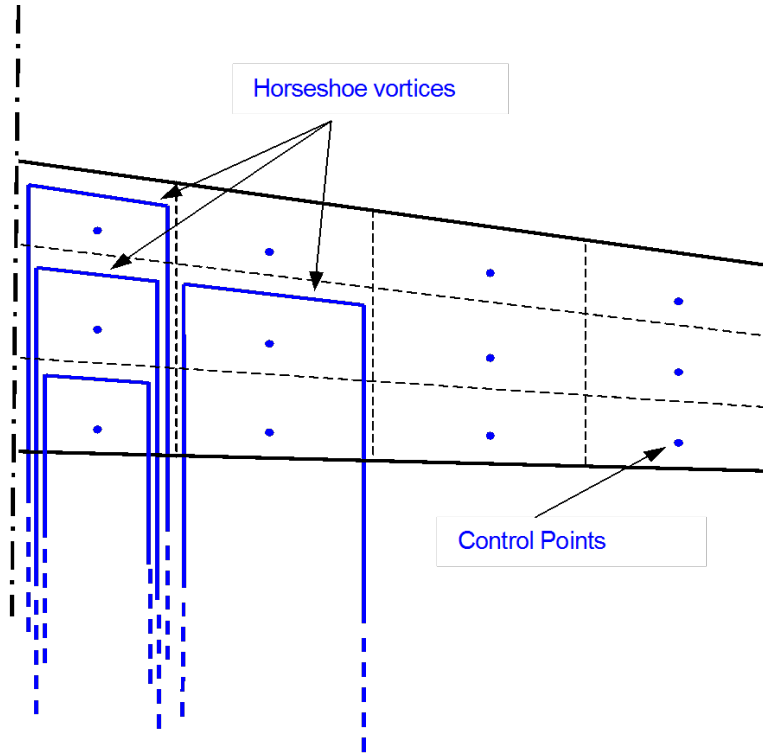


Figure 17: Classic VLM Method

In the method recommended by Katz and Plotkin [3], only the trailing vortices extend to infinity.

Since the wake must be force free, the strength of the trailing vortex is equal to that of the trailing edge quad vortex.

Both methods are implemented for comparison, but give close if not identical results in most cases.

**Panel disposition for VLM** The resolution of the system and the determination of the vortices' strengths require a matrix inversion. In some rare cases, this matrix may turn out to be singular due to a conflicting disposition of panels and control points on the wing's planform.

The problem arises when a control point is positioned on the line of a vortex. This will result in a division by zero. In those cases, manual re-paneling of the wing is sufficient to fix the problem.

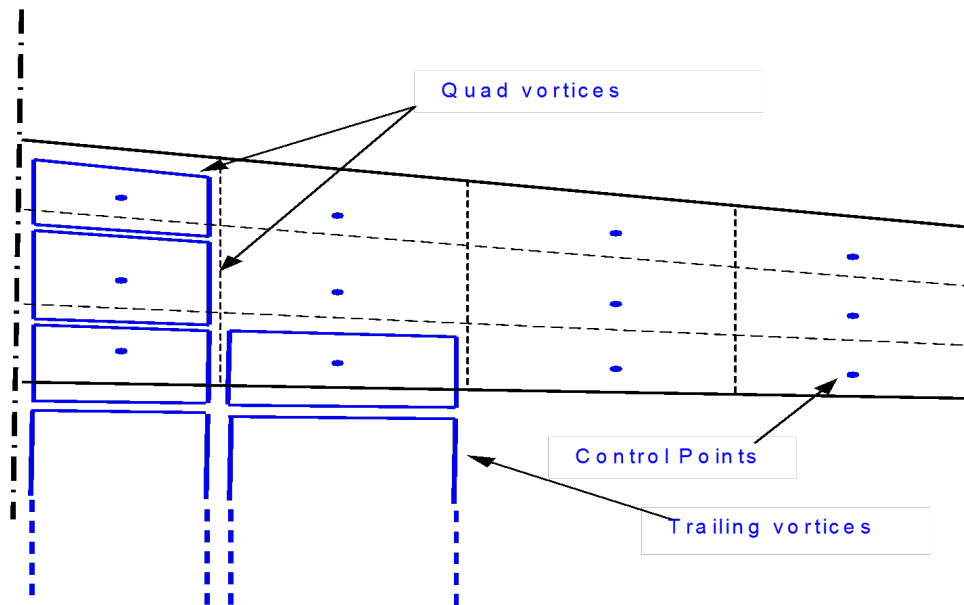


Figure 18: Quad VLM Method

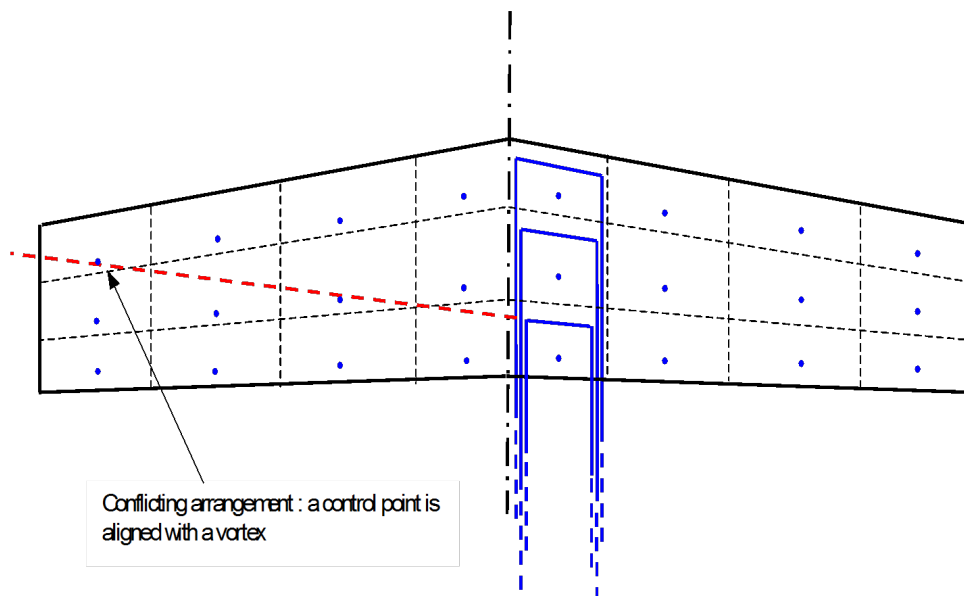


Figure 19: Quad VLM Method

---

If inversion problems persist despite re-paneling, it will be necessary to check the consistency of the input data.

#### 4.3.5 3D Panel Method - Linear

**General Principles** The 3D panel method has been implemented with the following objectives :

- refine the LLT and VLM results by a more sophisticated full 3D method, taking into account the wings's thickness, whereas the VLM only considers the mean camber line.
- provide insight in the  $C_p$  distributions over the top and bottom surfaces of a wing
- provide a method capable of modeling fuselages

The principle of a 3D Panel Method is to model the perturbation generated by the wing by a sum of doublets and sources distributed over the wing's top and bottom surfaces. The strength of the doublets and sources is calculated to meet the appropriate boundary conditions, which may be of the Dirichlet or Neumann type.

A comprehensive description of the principles of such a method is well outside the scope of this document. Only the main features necessary to a sound use of the code are detailed hereafter. The 3D method implemented in XFLR5 is essentially based on the method in reference [4]. For those interested, this document provides a comprehensive review of the theoretical and numerical aspects of the method.

**3D Panel method in XFLR5 v6** In XFLR5 v6, for a 3D-Panel type, the wing's are modeled differently depending on whether the analysis is run for a single wing or for a full plane :

- for the analysis of a single wing, the wing is modeled as thick surface, and the full 3D method described in 4 is applied
- for the analysis of a plane, the fuselage/body is taken into account, and the wings are modeled as thin surfaces; this is a restriction due to the impossibility to generate appropriate connections between wing and body without the help of a 3D-CAD program.

In reference [4], the authors propose to model the circulation on the wings using uniform strength doublets, and to place the Neumann type boundary condition at the collocation point, i.e. the panel's centroid or center of gravity. The alternative is to use a VLM method, and to place a vortex at the panel's  $1/4$  chord, and the BC point at the panel's  $3/4$  chord.

Both method have been tested, and the second alternative has proved more precise and reliable. Hence the 3D-panel method retained for planes is a mix model of uniform source/doublet for thick bodies, and horseshoe vortices for thin surfaces.

**Problem solving** The resolution of the panel problem requires the inversion of a square matrix of the size of the number of panels. This inversion is performed by LU decomposition.

**Wake roll-up** The wake roll-up process has been implemented and tested. However, it is not considered to be sufficiently robust to be released at this time, and has been disabled in v4.00.

**Boundary Conditions (BC)** In a VLM calculation, the BC are necessarily of the Neumann type, i.e. the velocity's component normal to the surface must be zero.

In a 3D-Panel calculation, the BC may be either of the Neumann or Dirichlet type. In the latter case the velocity's potential on the panel's inside surface is zero, so that the total potential inside the body is equal to the freestream velocity's potential.

After a trial and error process, the recommendation is to use Dirichlet BC rather than Neumann BC. The latter method is more sensitive to local geometry changes, and leads to less convincing results. This is also the choice which is implied in reference [4]. The type of BC can be modified in the "Advanced Settings" dialog box.

## Validation

**Infinite Cylinder and Sphere Analysis** The theoretical values for the  $C_p$  coefficients of a body in a uniform flow are :

- for a cylinder :  $C_p = 1.0$  at the leading and trailing edges, and  $C_p = -3.0$  at the lowest and highest points
- for a sphere :  $C_p = 1.0$  at the leading and trailing edges, and  $C_p = -1.25$  at the lowest and highest points

These values are calculated within % by the 3D panel analysis.

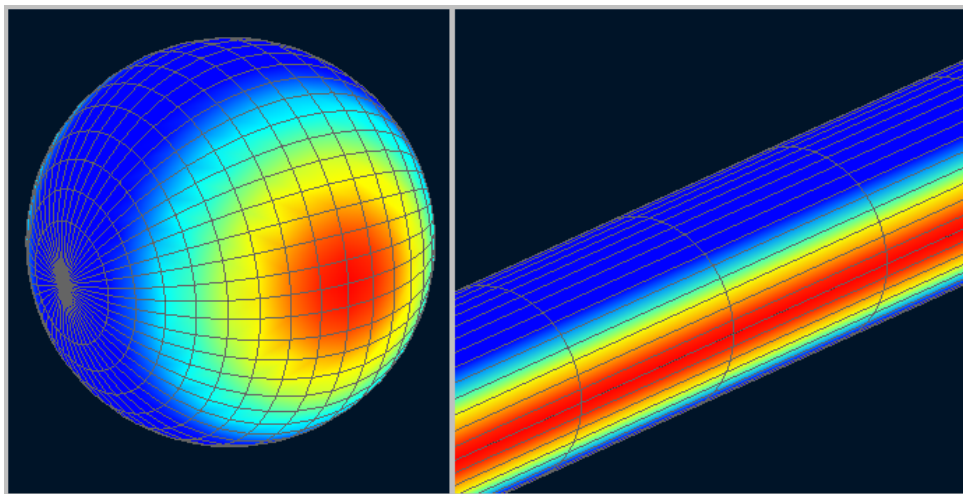


Figure 20: Pressure coefficient Analysis – Sphere and near infinite cylinder

**Wing Analysis** The  $C_p$  distributions calculated by 3D panel analysis for a near infinite wing, and by 2D panel analysis with XFOIL are plotted in Figure 22 and in Figure 23. There is general concordance for inviscid results.



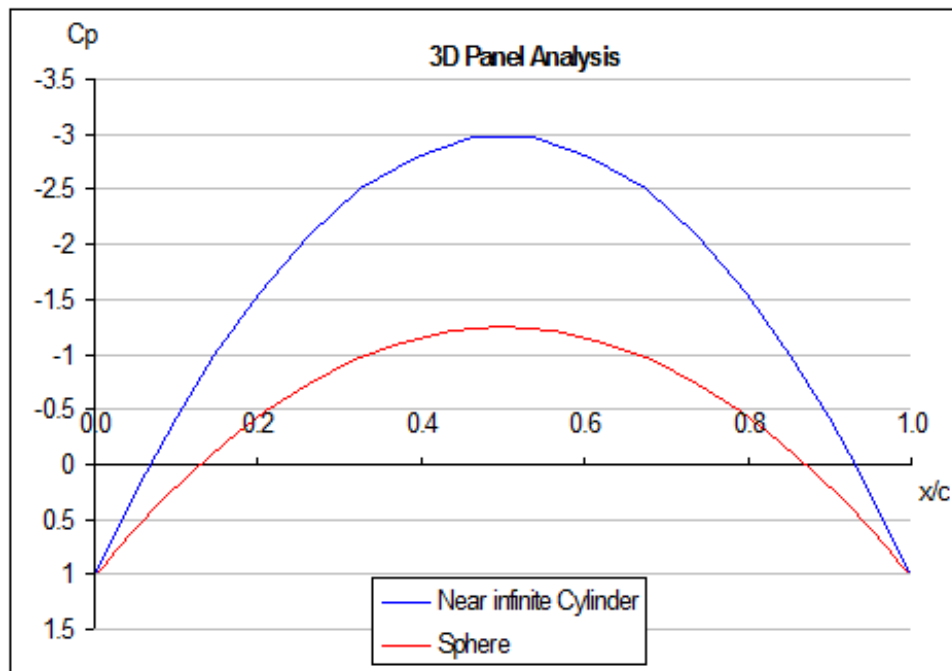


Figure 21: Pressure Coefficient Analysis – Sphere and near infinite cylinder

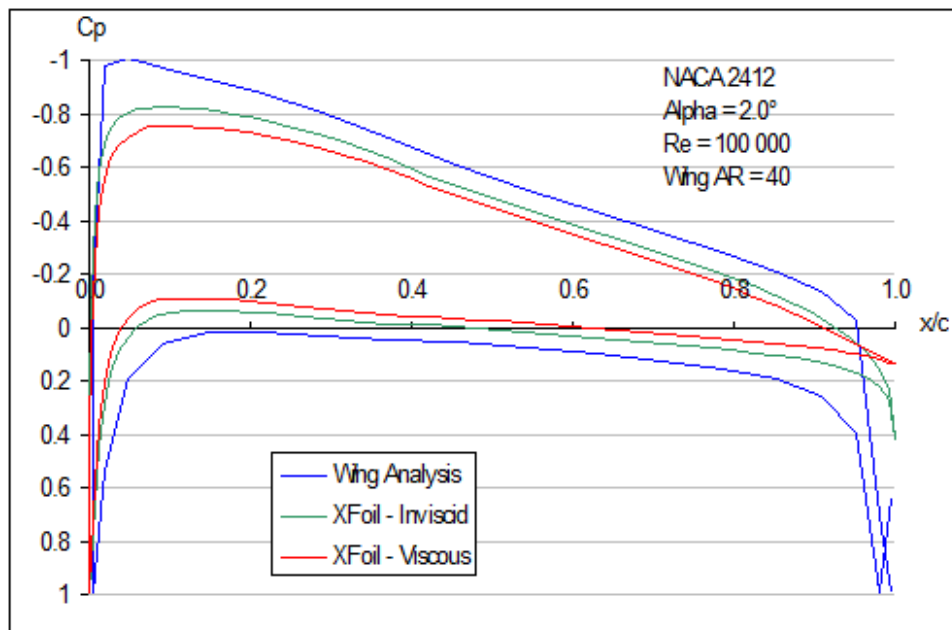


Figure 22: Pressure Coefficient Analysis – NACA2412

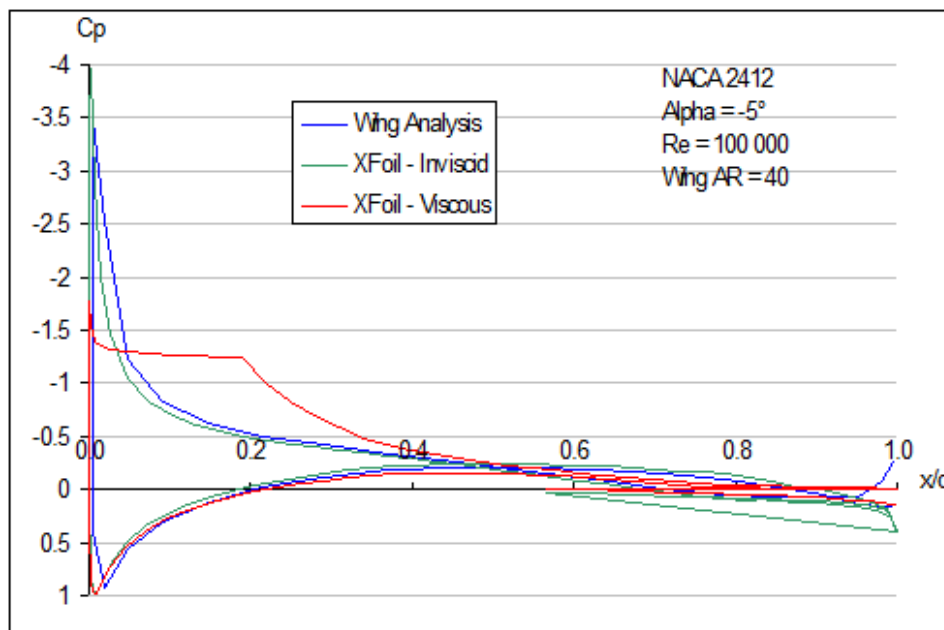


Figure 23: Pressure Coefficient Analysis – NACA64A410

#### 4.3.6 Analysis considerations

**General Limitations** As a general rule, LLT and VLM are adapted to configurations of thin lifting surfaces, operating at small angles of attack.

The most questionable assumption of the wing design algorithm is probably the use of XFOIL transition results to wings with finite aspect ratio. The 2D simulation proposed by XFOIL corresponds to infinite wings, where a laminar bubble extends indefinitely along the span. Some authors suggest that on span-limited wings, such bubbles will appear only on a fraction of the planform. However, theories for 3D transitions are still in development and to the author's knowledge, not giving total satisfaction yet.

The method which consists in interpolating XFOIL generated results is clearly an approximation with no real theoretical or experimental background, but should be a reasonable approximation for wings with moderate to high aspect ratio.

The viscous characteristics will be less and less representative as the wing geometries differ from the ideal 2D Xfoil infinite wing. Hence those results for non planar geometries, low aspect ratio or high sweep should be considered with caution.

**Selection of an Analysis Method** The LLT method should always be preferred if the wing's geometry is consistent with the limitations of the theory. LLT provides better insight into the viscous drag, gives a better estimation of the behavior around stall conditions at high angles of attack, and is better supported by theoretical published work. The 3D panel method should be selected if there is interest in the  $C_p$  distribution on top and bottom surfaces, or if the body's influence should be taken into account.

VLM analysis is preferable for all other cases.

The comparison of the  $C_p$  distribution at two span positions for different method of analysis is given in Figure 24 and Figure 25.

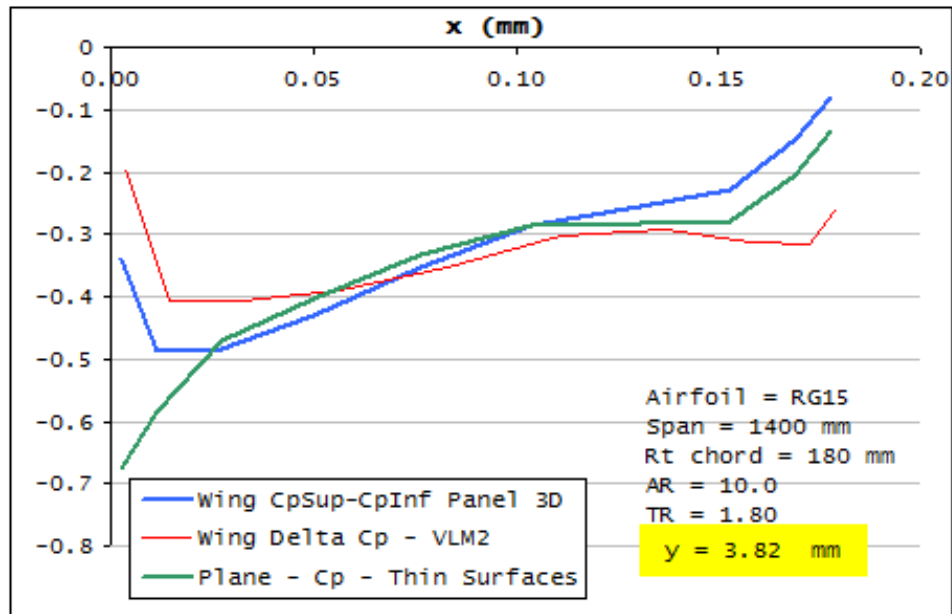


Figure 24: Cp comparison for different analysis methods

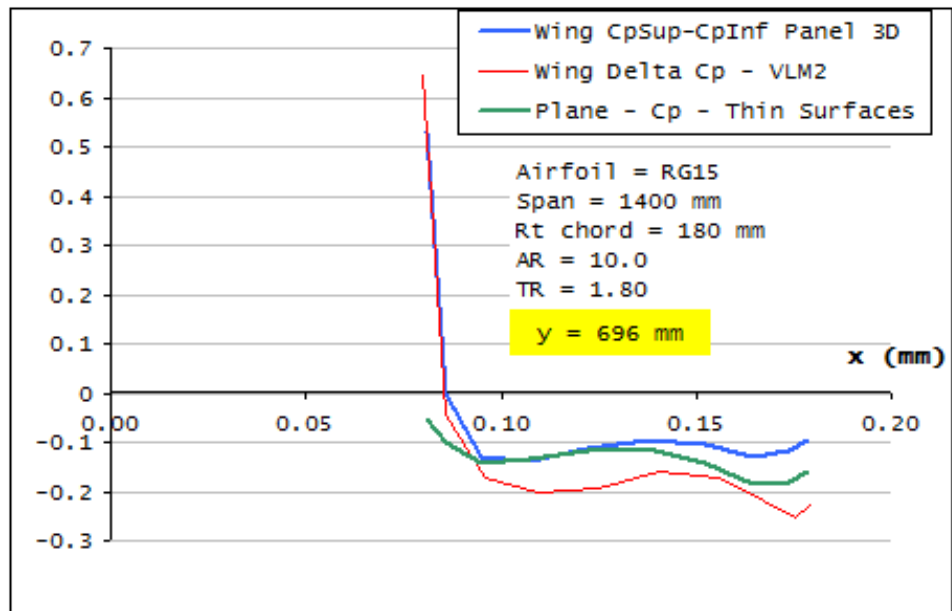


Figure 25: Cp comparison for different analysis methods

**Core radius** In VLM analysis, the velocity vector induced by a vortex is singular on the vortex line.

In a 3D panel method, the velocity vector is singular in the alignment of the panel sides. This can create numerical errors in the analysis and in the calculations of the streamlines. It is therefore highly recommended to set a minimal core radius, which can typically be of the order of magnitude of 1/1000 of the min mesh panel size, e.g.  $Coreradius = 10^{-6}m$ . This is the value set by default, and it can be modified in the advanced settings.

The velocity at a point located on the vortex line, or in the alignment of a panel side, is zero.

**Sideslip** The simulation of sideslip has been introduced in XFLR5 v4.09.

The order in which a.o.a. and sideslip are applied has its importance. In XFLR5, sideslip is modeled by rotating the model about the z-axis, with a freestream velocity vector remaining in the x-z plane. The resulting geometry is analyzed using the conventional VLM and panel methods. The advantage of this method is that the trailing vortices are in the vertical plane which contains the velocity vector, i.e. are aligned with the x-axis of the stability frame.

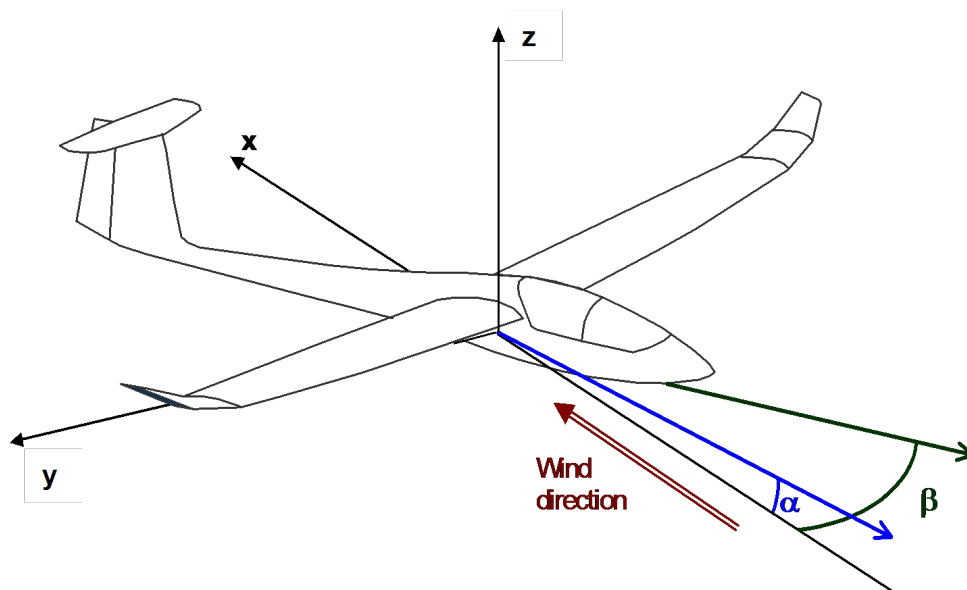


Figure 26: Definition of sideslip

**Trefftz Plane, far field and near field analysis** The lift and induced drag may be calculated by near field or by far field methods. The theoretical aspects are too vast to be detailed here, but in essence the near field method consists in an integration of pressure forces on the panels, whereas the far field method is based on the balance of the momentum on a control surface far downstream of the body, i.e. the Trefftz plane.

It is generally reported that the drag and lift results from near field analysis are significantly higher and less representative than those resulting from a calculation in the Trefftz plane. This issue is not specific to the present implementation, but is reported for almost all VLM and panel codes. The implementation in the present code for the calculation of lift and drag is therefore the far field method.

On the other hand, far field analysis does not provide information on the pressure distribution over the strip, and no information on the pitching moment with reference to the chord's quarter point. All the moments and the position of the center of pressure are therefore calculated by summation on the panels.

In the current implementation of the 3Dpanel method, it is considered that only the wings shed a wake, and that the body does not.

**Linear and non-linear behavior** Traditional VLM and Panel analysis do not account for viscous effects. For model aircraft operating at a few m/s however, the viscous drag is not negligible compared to the induced drag, and must therefore be estimated by an alternative mean.

In the present application, the viscous drag is estimated by interpolation of Xfoil pre-generated polars, by the  $C_l$  value resulting from the linear 3D analysis. This assumes implicitly that the foil's behavior on a finite wing is not very different than on an "infinite Xfoil wing". There is no real background, neither theoretical nor experimental, to support this approach, so it should be used with caution.

As is generally the case when transposing 2D results to 3D analysis, the estimation of viscous drag is probably too low and may lead to arguably optimistic results.

Because the VLM is linear, it does not, among other things, account properly for stall at high angles of attack, unlike, potentially, the LLT.

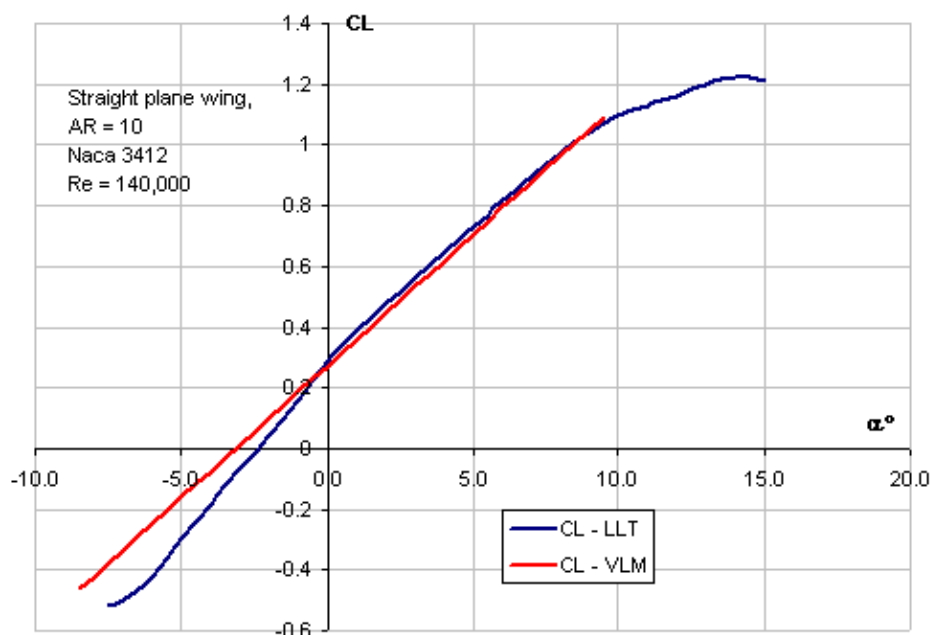


Figure 27: Linear and Non-Linear modeling

## Non-Linear Implementation

**Tilted Geometry – VLM and 3D Panel Analysis** The baseline VLM method uses small angle approximation for the wake's definition. Within this assumption, the wake is aligned with the body axes :

Wing definition
VLM Mesh creation
Selection of $\alpha$ , $V_\infty$ parameters
Creation of the vortex influence matrix and of the boundary conditions
Inversion of the matrix for the vortices strength $\Gamma_i$
If Type 2 analysis, scaling of $V_\infty$ and of the $\Gamma_i$ to create a lift opposite to the weight
Calculation of the induced downwash and induced angles in the Trefftz plane
Calculation of the Cl values from the $\Gamma_i$
Calculation of the induced drag in the Trefftz plane
Interpolation from Cl on the type 1 polar mesh of the other viscous variables VCD, transitions, etc.

- 
- For VLM, the trailing legs of the horseshoe vortices are parallel to the body's x-axis (Figure 28a).
  - For 3D Panel analysis, the trailing wake panels are in the x-y plane

The advantage of this approximation is its simplicity : only one influence matrix is required for all angles of attack, and the matrix inversion can be performed for all alphas simultaneously.

The disadvantage is that the horseshoe vortices or the wake panels are not aligned with the freestream velocity.

A more representative approach is to align the wake with the wind axes (Figure 28b). Equivalently, the problem can be set in the wind axes and the body's geometry can be tilted by the angle of attack (Figure 28c), which is a direct transposition of the physics of the problem. Both methods are equivalent, but the latter can be implemented more simply, hence has been chosen for XFLR5. It is selected by checking the "Tilt Geometry" checkbox in the Analysis Dialog Box.

The inconvenience with this approach is that a new matrix must be set up and inverted for each angle of attack, leading to longer computation times.

The coefficients  $C_l$  and  $C_d$  are almost identical for both methods, which means the small angles approximation is applicable from the performance analysis point of view. The moment coefficients may be slightly different.

**Wake roll-up – VLM and 3D Panel Analysis** Note : Because it is sensitive and difficult to use, the wake roll-up process has been disabled. The following explanation is provided for information only.

**General considerations** In their base formulation, both the VLM and the Panel methods make the assumption of a flat wake, which is an approximation. The wake tends to roll up on itself, which can be illustrated for instance by the two vortices at the tip of each wing.

A wake model more refined than the simple straight line or flat panel can be of interest for two reasons :

- Although the wake carries no load and therefore has no influence on the lift coefficient, its shape affects the induced drag value and derived coefficients
- A flat wake is inappropriate for plane configurations with and elevator, since the downwash created by the main wing influences the flow field around the elevator.

The shape of the wake is determined by the flowfield behind the wing, but in turn, the flow field is dependent on the wake shape. Therefore, the shape the wake takes in a constant state situation can be deduced by an iterative process, in which the wake geometry is updated ("relaxed") after each computation loop.

**Wake mesh** The panels formulation implemented in XFLR5 is of the constant, flat panel type. Special care must therefore be taken in the choice for the wake panel's size, to avoid excessive twisting. The panel size is controlled by three parameters :

- The wake's total length

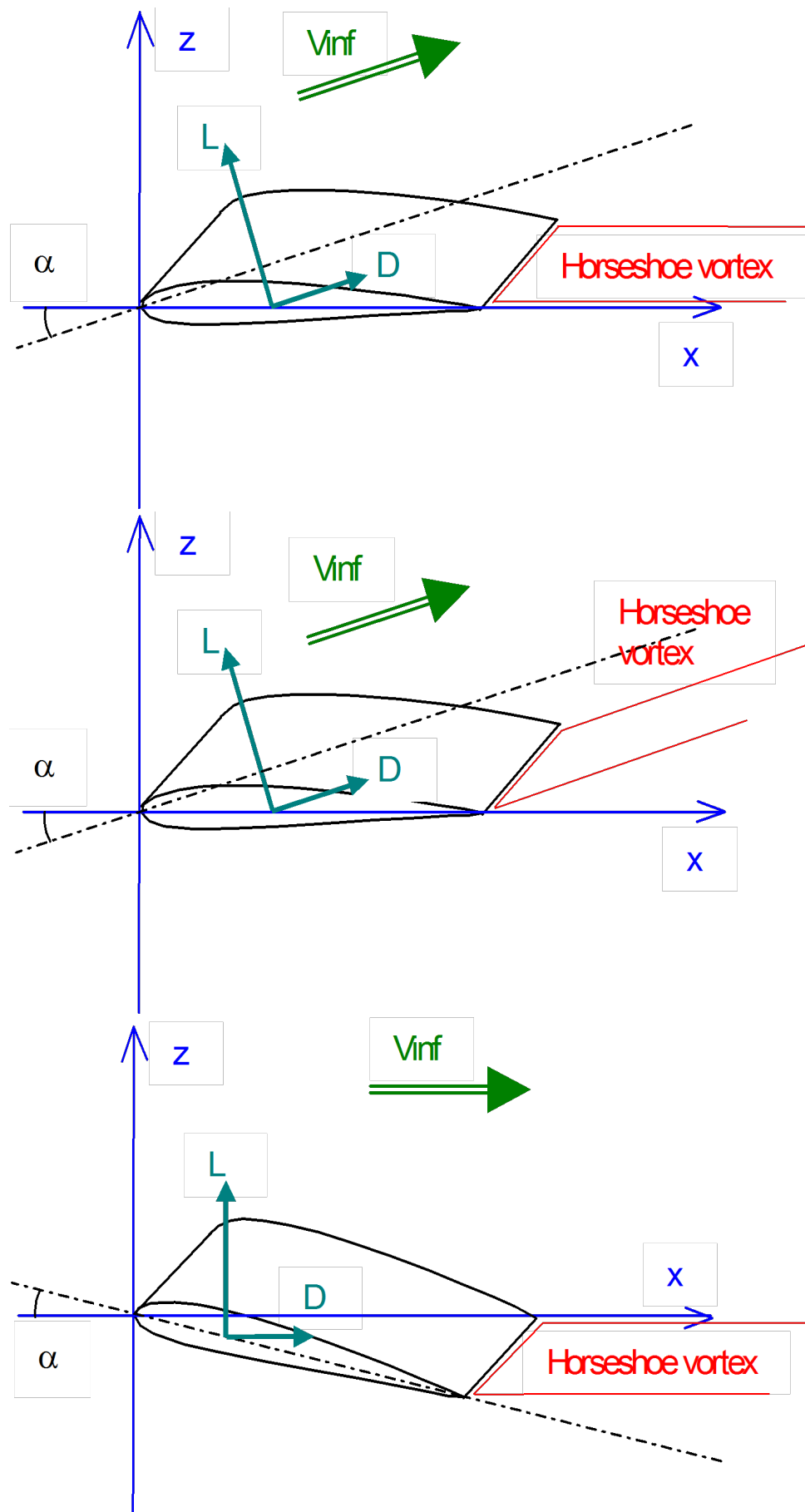


Figure 28: Normal and Tilted geometry configurations



- The streamwise size for the first wake panel's length
- The ratio, or progression factor, between two adjacent panels in the streamwise direction

As a general indication, it is advisable to set those parameters so that the first panel's size is approximately the same as that of the wing's trailing edge panel.

**Roll-up process** Ideally, the lift and drag coefficients tend towards limit values. However, if no special precautions are taken, numerical experiments show that the wake tends to roll up indefinitely on itself. This leads to highly twisted panels and to numerical divergence.

Since the roll-up is not a robust process, the iteration loop is limited both by the number of iterations and by a precision criterion.

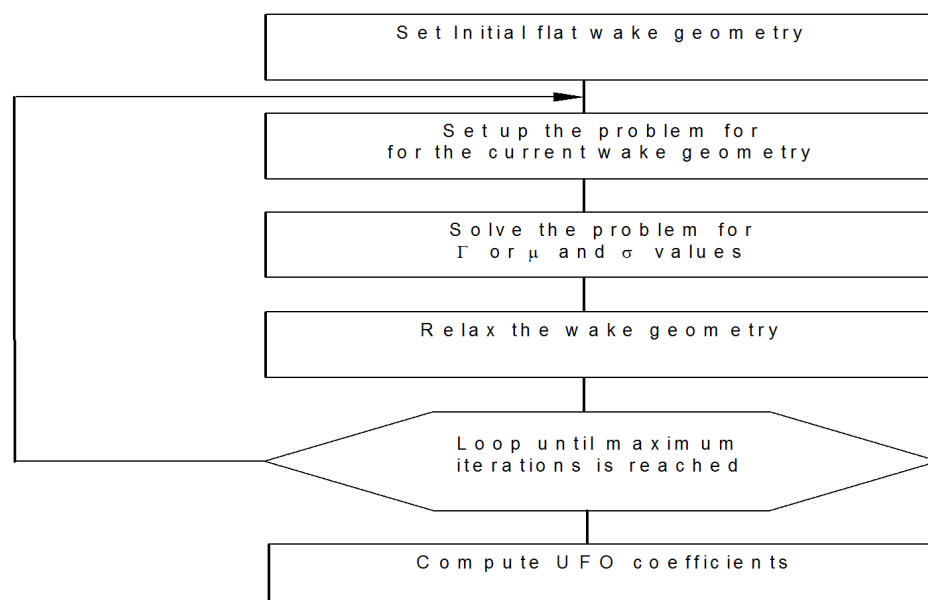


Figure 29: Wake roll-up iteration process

Reference [5] provides a comprehensive description of the issues related to wake roll-up.

### 4.3.7 Moments

All moment calculations in LLT are strictly in accordance with the formula of NACA TN1269.

In V4.00, the definition of the moments has been modified to clarify some ambiguities that existed up to v3.21.

From V4.00 onwards, the geometric pitching, rolling and yawing moments are calculated by integration of forces on the panels. For VLM this is done at the vortex middle position, for 3D Panel analysis, the force is applied at the panel's center.

The geometric moments are therefore the total moments applied to the wing or plane.

For analysis purposes, it may be interesting to break down those moments in separate parts, or to isolate one specific contribution to the total moment.

#### Strip Moment Coefficients

These moments are calculated for each span position on the wing and are accessible in the Operating Point graphs.

Moment		Sign	Ref. Len.	Nature	LLT	VLM & 3D Panel
Pitching	Airfoil $C_m$ Airfoil	positive nose up	M.A.C : $M = q.S.mac.C_m$	Moment of the lift forces around the 1/4 chord point	The value for the pitching moment is interpolated on the foil's polar mesh. It takes into account viscous effects	Sum of the moments created by pressure forces on the strip's panels. The viscous part is ignored
	$C_m$			Moment of the pressure and viscous forces with respect to XCmRef	Integration over the wing's lifting line of the strips self pitching moment, and of the strip lift force. Both sweep and dihedral are taken into account	Sum on all the panels of the moments of pressure forces + pitching moment of viscous drag forces

Table 1: Strip Moment Coefficients

### Wing moment coefficients

#### 4.3.8 Neutral point, Center of pressure, Static Margin

XFLR5 up to v3.12 has provided a measure of the quantity

$$SM = \frac{(X_{CP} - X_{CG})}{MAC}$$

incorrectly labeled "Static Margin", where

- $X_{CP}$  is the centre of pressure's streamwise position
- $X_{CG}$  is the centre of gravity's streamwise position

The conventional static margin of a wing or a plane may be determined by an iterative process. It is the CG position (or moment reference position XCmRef) for which

$$\frac{dC_m}{d\alpha} = 0$$

This is illustrated in the Figure 30 where the neutral point is approximately 67 mm from the leading edge.

Illustration of the way to use XFLR5 to position the CG of a model sailplane are given in [6] and [7].

#### 4.3.9 Efficiency factor

The efficiency factor, referred to also as Oswald's factor, is a measure of the deviations of the wing's induced drag from that of an optimal elliptic loading, and is defined as

$$e = \frac{CL^2}{\pi \cdot AR \cdot ICd}$$

where

Moment		Sign	Ref. Len.	Nature	LLT	VLM & 3D Panel
Pitching	Geom (global) $GCm$ Airfoil	positive nose up	M.A.C : $M = q.S.mac.C_m$	Moment of the pressure forces with respect to XCmRef	Integration of the moment over the wing's lifting line. Both sweep and dihedral are taken into account	Sum on all the panels of the moments of pressure forces
	Viscous (global) $VCm$			Moment of the viscous airfoil drag forces with respect to XCmRef	Integration of the moment over the wing's lifting line.	
	Airfoil (at local span pos.)			Moment of the lift forces around 1/4 chord point	Cm interpolated on polar 1 mesh	Sum of the moments created by pressure forces on the strip's panels
Rolling	Geom (global) $GRm$	positive with the starboard wing down	Span : $R = q.S.b.C_r$	Moment of the pressure forces with respect to XCmRef	Integration of the lift's moment over the wing's lifting line. Dihedral is not taken into account	Sum on all the panels of the moments of pressure forces
Yawing	Geom (global) $GYm$	positive with the nose to starboard	Span : $N = q.S.b.C_n$	Moment of the pressure forces with respect to XCmRef	N/A	Sum on all the panels of the moments of pressure forces
	Profile (global) $VYm$			Moment of the viscous airfoil drag forces with respect to the plane $y=0$	Integration of the moment over the wing's lifting line	
	Induced (global) $IYm$			Moment of the induced tangential forces with respect to the plane $y=0$	Integration of the moment over the wing's lifting line	

Table 2: Wing moment coefficients

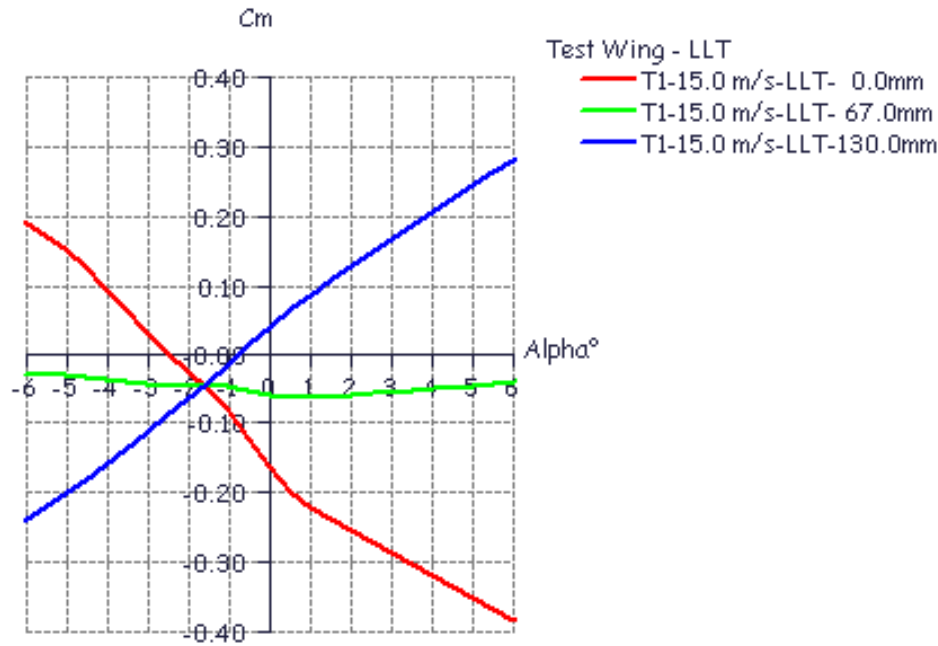


Figure 30: Wing Neutral Point

- CL is the lift coefficient
- ICd is the induced drag coefficient
- AR is the wing's Aspect Ratio

The efficiency factor, also named Oswald's factor, should always be smaller than 1. It may happen however that this factor becomes greater than 1 for numerical reasons in LLT, VLM and 3D Panel calculations.

In LLT, this may be corrected by increasing the precision required for convergence, for instance with the following parameters :

- Number of stations = 40
- Relaxation factor = 40
- convergence criterion = 0.001
- Max Number of iterations = 300

In VLM and 3D Panels, a refinement of the panel density in the streamwise direction is required to reduce the efficiency factor to values less than 1.

#### 4.3.10 Wing Operating Points and Wing Polars

The presentation of results is the same as for foil analysis, i.e. each converged analysis generates an operating point and adds results to a polar object. The definition and selection of an Analysis/Polar object is necessary to perform a calculation.

Any number of Operating Points may be stored in the runtime database, the only limitation being computer memory. Wing and plane operating points will use significant memory resources.

Type 1 and Type 4 polars are unchanged from foil analysis.

A type 2 polar corresponds to a plane with a given weight operating at constant lift.

For a given angle of attack, the plane's velocity is calculated to create a lift force opposite to the weight of the airplane :

$$V = \sqrt{\frac{2mg}{\rho SC_l}}$$

The angle of descent is

$$\gamma = \arctan\left(\frac{C_d}{C_l}\right)$$

and the horizontal and vertical speeds are respectively

$$V_x = V_\infty \cos(\gamma)$$

$$V_z = V_\infty \sin(\gamma)$$

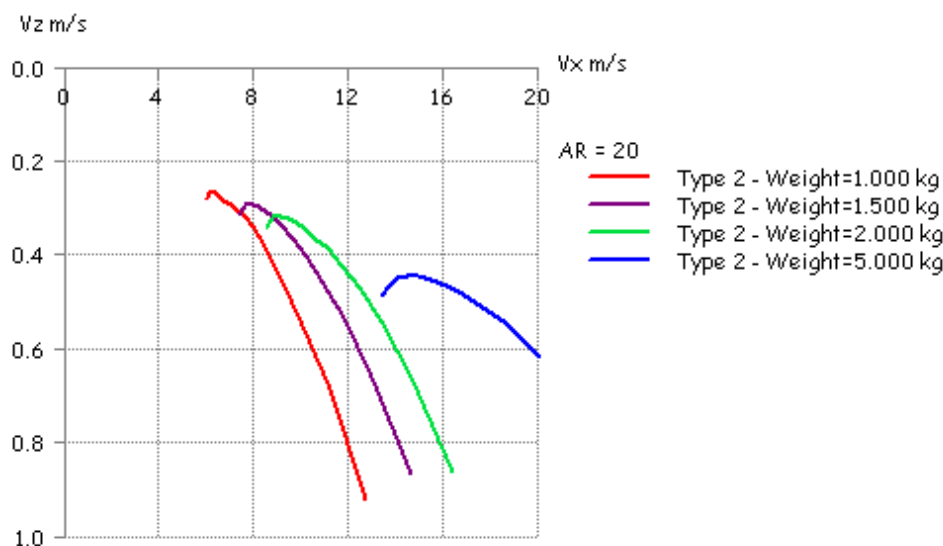


Figure 31: Speed polars based on Type 2 analysis

Convergence for type 2 polars requires that the apparent angle of attack be greater than the zero-lift angle. Otherwise, no speed whatsoever may generate a positive lift...

#### 4.3.11 Control analysis – Polar Type 5 and Type 6

The Type 5 and Type 6 control polars have been disabled in XFLR5 v6 and are replaced by the Type 7 stability polars.

#### 4.3.12 Interpolation of the Xfoil-generated Polar Mesh

The code does not recalculate with Xfoil each operating point at every wing station and at each iteration:

- this would require lengthy -and unnecessary- calculations
- XFoil's convergence is too uncertain

Instead, the operating point is interpolated from a pre-generated set of Type 1 polars. The wing calculation requires that a set of **Type 1** foil polars be previously loaded or generated for each of the wing's foils.

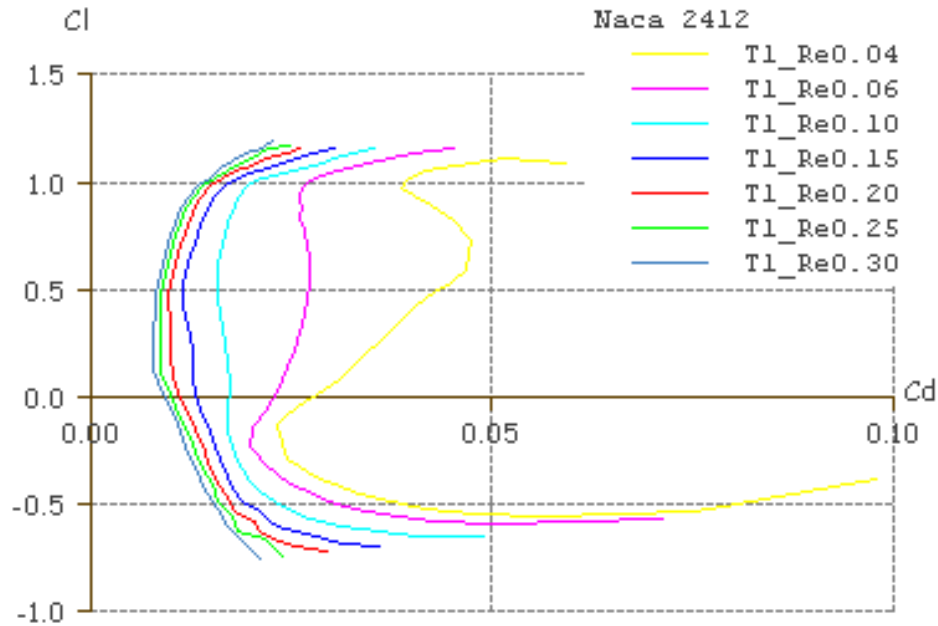


Figure 32: Polar mesh ranging from  $Re = 40,000$  to  $Re = 300,000$

The set of polars should cover the whole flight envelope of each point of the wing, with regard to both Reynolds numbers and to the apparent angle of attack.

If any point of the wing planform operates outside the available polar mesh, a warning message is issued in the log file. This happens for instance in the case of short tip chords of elliptic wings. In such a case, the "closest point" of the mesh will be used, and the operating point may be generated and added to the current polar, if so chosen by the user.

For the interpolation process, the code uses indifferently all available type 1 polars related to the selected foil. The user must therefore be careful to provide only a homogeneous and consistent set of polars.

The interpolation process of a variable  $X$  ( $X$  being  $Cl$ ,  $Cd$ ,  $Cm$ , Transition points etc.) from  $[\alpha = aoa + \alpha_i + washout, Re]$  at a geometrical point  $P$  between the foils 1 and 2 is:

1. For the first foil, find polars 1 and 2 such that  $Re_1 < Re < Re_2$ ;  
if neither polar 1 nor 2 can be found, return on error  
if  $Re$  is less than all the polars' Reynolds numbers, use the polar of smallest  $Re$   
if  $Re$  is greater than that of any polars' number, use the polar of greatest  $Re$
2. Interpolate each polar with  $\alpha$  to get  $X_{11}$  and  $X_{12}$   
if either polar is not defined up to  $\alpha$ , use the smallest or greatest angle available,

---

and issue a warning

if only one polar is available, interpolate only that polar, and issue a warning

3. Interpolate  $X_1$  between  $X_{11}$  and  $X_{12}$ , pro-rata of  $Re$  between  $Re_1$  and  $Re_2$
4. Do the same for the second foil to get  $X_2$
5. Interpolate  $X$  between  $X_1$  and  $X_2$ , pro-rata of the position of the point between the two foils

#### 4.3.13 Streamlines

The streamlines are calculated from the vortices, or doublet and source, strengths each time an operating point is selected.

The calculation is incremental, in the x streamwise direction.

The streamline are initiated at the mesh panels leading edge or trailing edge, with a user defined offset in the x and z directions.

The "Initial Length" is the first x-increment for the calculation of the streamline.

The "Progression Factor" determines the length of step n+1 vs. step n.

Caution note : The velocity vector is singular at the panel edges in 3D-Panel analysis, and on the panel's vortex trailing line in VLM analysis. This may cause numerical instabilities, in cases for instance when the streamlines are requested to initiate exactly at the panels leading or trailing edge, or at the panel corners. A minor x or z offset is necessary to prevent the instability. The use of a core radius, which can be defined in the advanced settings, is another possibility.

#### 4.3.14 Comparison to experimental results

The code has been tested against experimental results and against other software, with consistent results.

Also, the VLM, 3D Panel and LLT algorithms in their XFLR5 implementation are totally independent, but give close results in the linear part of the  $Cl$  vs.  $\alpha$  plots.

#### 4.3.15 Comparison to wind tunnel data

An experiment has been carried out beginning of 2008 on a model sailplane. The detailed results are given in [9].

The following figures provide results from XFLR5 v3.21 and from v4.09. Results from v3.21 are marked as "FMe", since the calculation has been performed by F. Meschia.

Note : in v4.09, the lift calculation was performed by integration of pressure forces on the panels. From v4.13, the calculation is performed in the far field plane.

It can be concluded that

- the VLM is at least as reliable as the 3D panel method,
- the body modeling does not improve the precision of the results
- both methods give reasonable estimations of values such as :
  - lift coefficient
  - zero lift angle

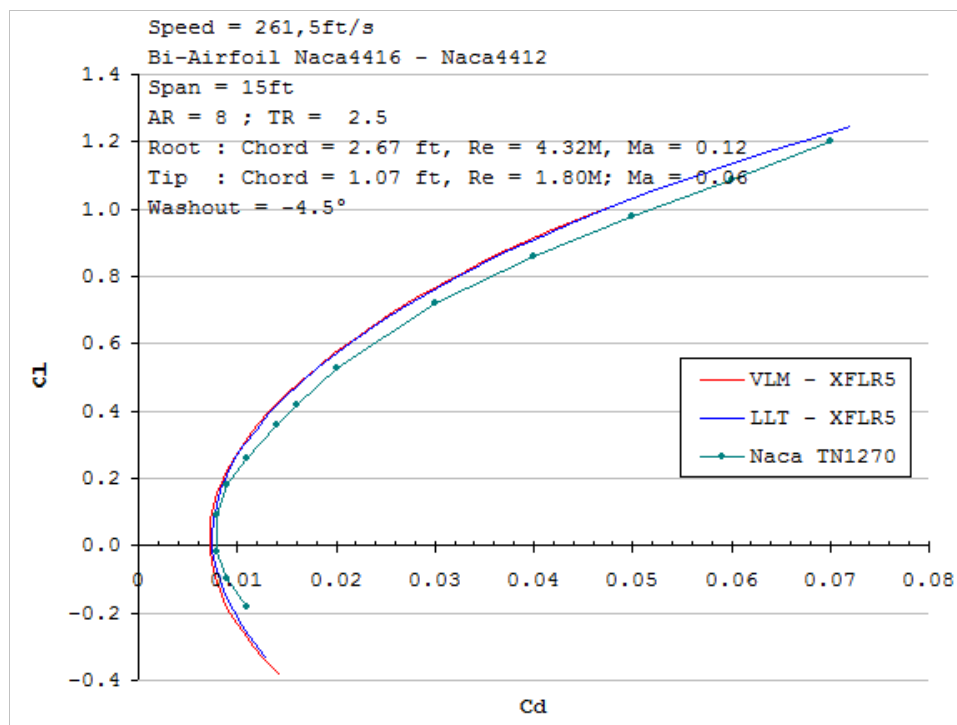


Figure 33: Comparison to test results from Naca Tech. Note 1270

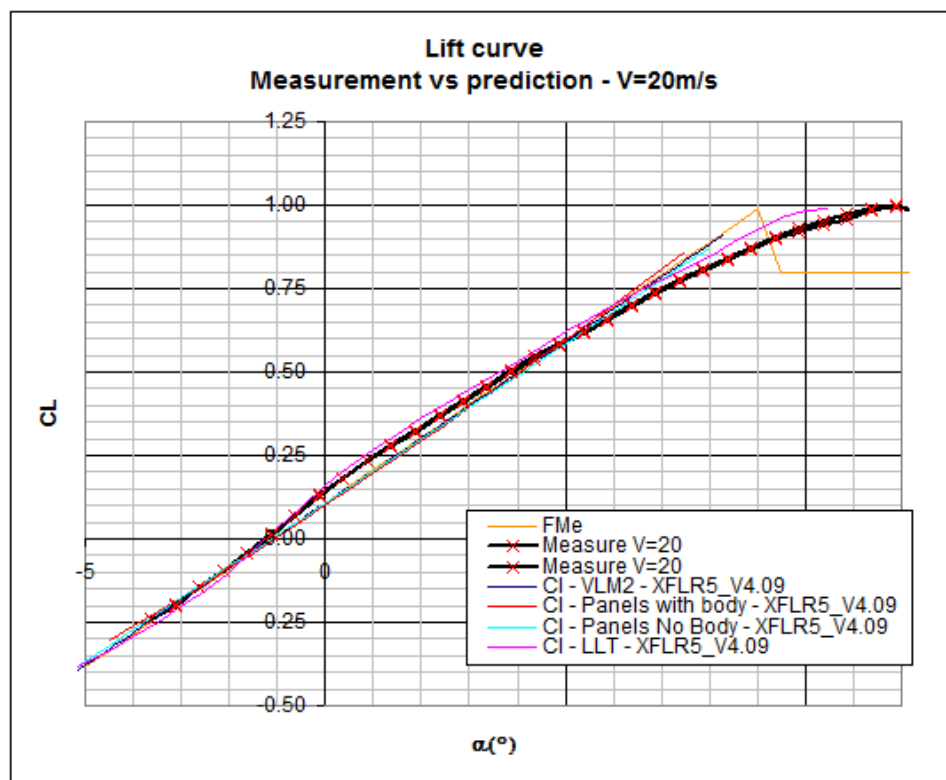


Figure 34: Predicted lift curve vs. experimental results



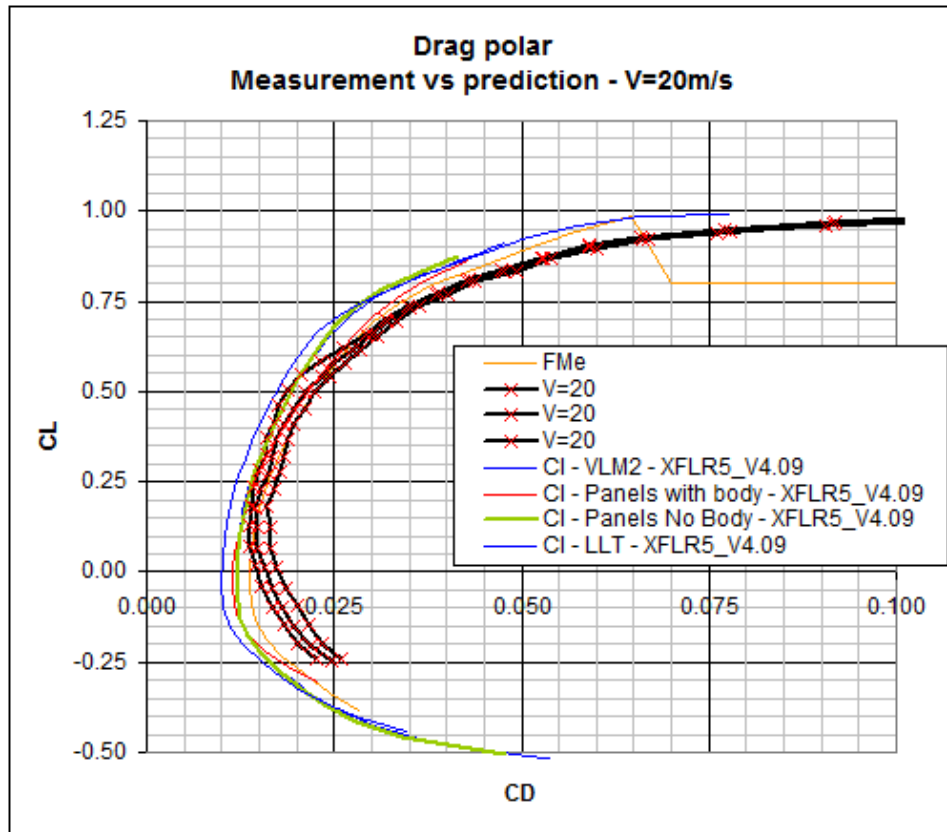


Figure 35: Predicted drag polar vs. experimental results

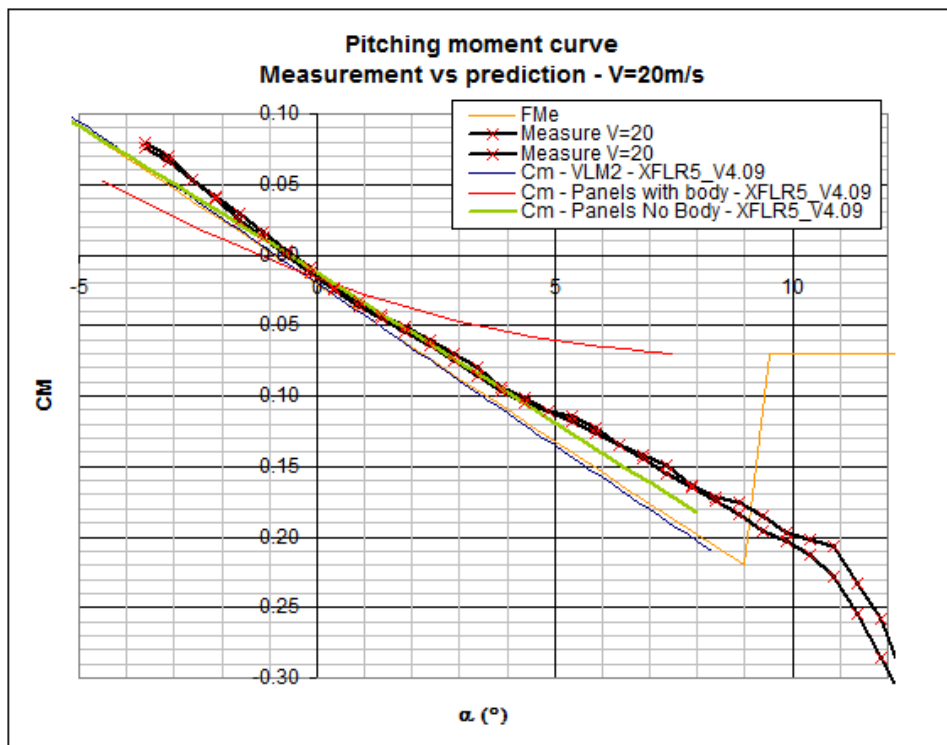


Figure 36: Predicted pitch moment vs. experimental results

- pitch moment coefficient
- zero lift moment or zero moment lift
- both methods tend to underestimate the drag, probably the viscous part of it

#### 4.3.16 Comparison to Miarex and AVL results

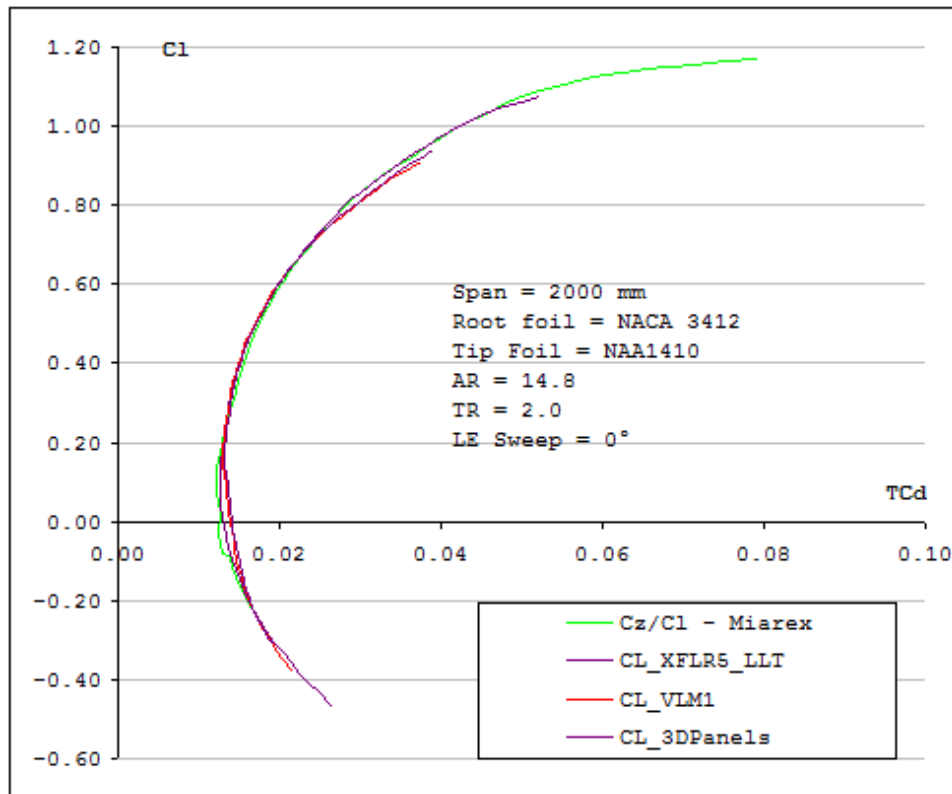


Figure 37: Comparison to results from Miarex

Note about induced drag : the heterogeneity of AVL results is unexplained.

#### 4.3.17 Session example – Wing Analysis

1. Load the foil(s) which will be used to define the wing
2. In the Direct Analysis Application, click the "Run Batch Analysis" command in the Polars menu, or type **Shift ↑** + **F6**
3. Run a batch analysis with the following parameters (make sure these values cover the whole flight envelope of the wing):
  - from  $\alpha = -6^\circ$  to  $\alpha = 10^\circ$
  - from  $Re = 40,000$  to  $Re = 160,000$  every 20,000
  - from  $Re = 200,000$  to  $Re = 500,000$  every 50,000

or use a predefined list Checking the box "Start from zero" will cause the analysis to start from  $\varpi = 0^\circ$ , going upwards to  $\alpha_{max}$ , then downwards to  $\alpha_{min}$  this usually facilitates convergence

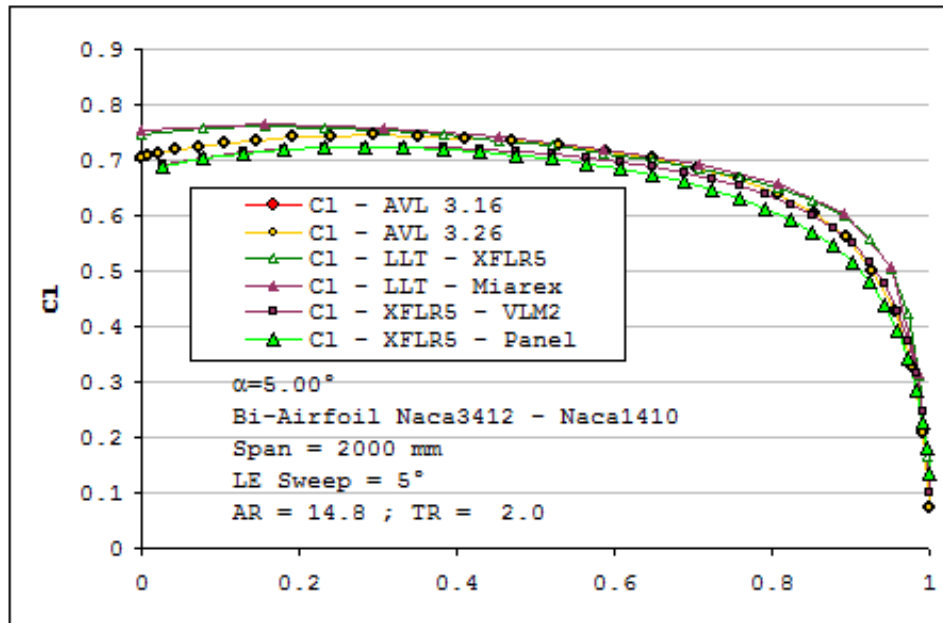


Figure 38: Lift coefficient - Comparison to AVL and Miarex

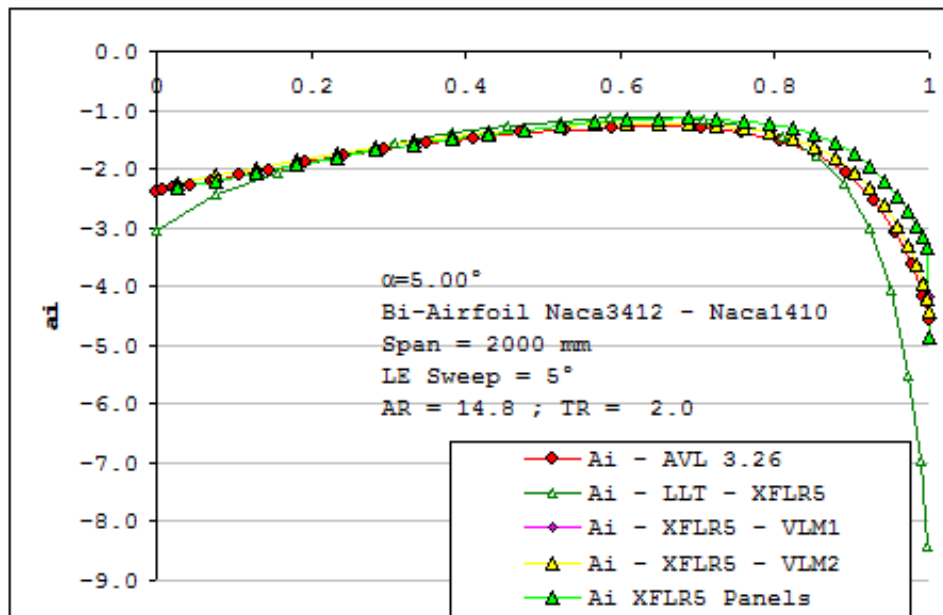


Figure 39: Induced Angle vs. span - Comparison to AVL and Miarex

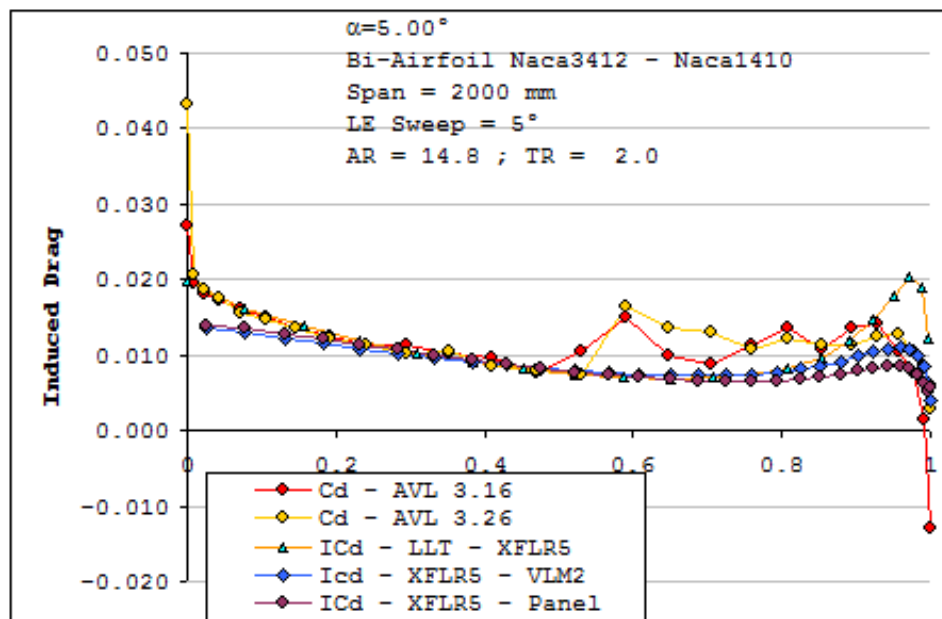


Figure 40: Induced Drag vs. span - Comparison to AVL and Miarex

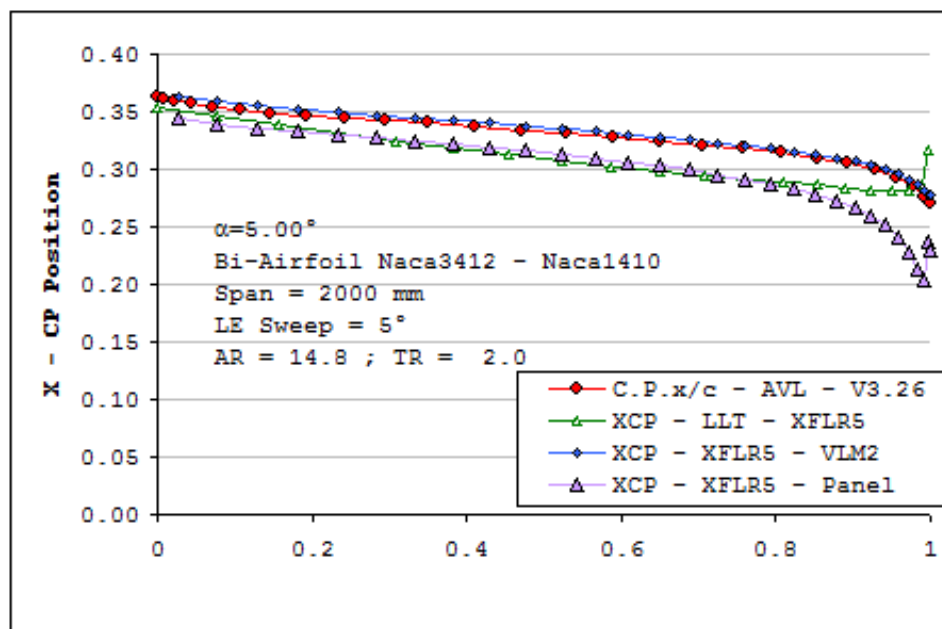


Figure 41: Center of pressure position vs. span - Comparison to AVL and Miarex

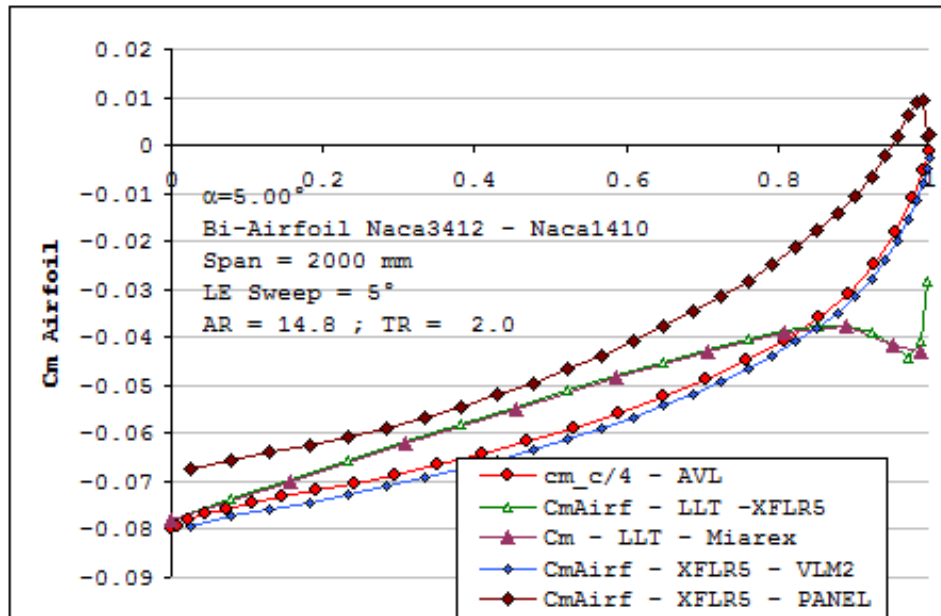



Figure 42: Pitching moment coefficient vs. span - Comparison to AVL and Miarex

4. Close the dialog box
5. Optional : Use the "Save Associated Polars" in the "Current Foil" menu to save the polars to a ".plr" file for use in future projects
6. Switch to the Wing Design Application **[Ctrl]** + **[6]**
7. Click the "Define Wing" command, **[F3]** in the Wing menu, or "Define a Plane" (**[Ctrl]** + **[F3]**)
8. Define the object and close the dialog box
9. Optional, but recommended : Define the inertia properties of the current plane or wing object.
10. Select Current plane(or wing)/Define Inertia
11. Enter the inertia properties for the plane or wing.
12. Make sure that the CoG position is where it's meant to be. It may be necessary to "cheat" a little on the positions of point masses to achieve the desired position
13. Close the dialog box
14. Click the "Define Analysis/polar" in the Wing Polar menu, (**[F6]**)
15. Activate the Type 2 check box
16. Define the plane mass and the center of gravity position (the moment ref. location), or select the option to use the plane's inertia
17. Unless the wing has either low aspect ratio, high sweep, or high dihedral, select the "LLT" checkbox, and close the dialog box (**[←]** and **[←]**)

18. Leave the LLT settings to the default values in the "Operating Point" menu, i.e. "Relax Factor = 20" and "N° of Stations Along the Span = 20"
19. Select an angle of attack in the right toolbar which can be expected to give positive lift equal to the model weight at reasonable Speed/Re values – for instance  $\alpha = 3^\circ$
20. Click the "Analyze" button in the right toolbar
21. Change settings if LLT convergence cannot be reached, or continue the LLT analysis after un-checking the "Init LLT" checkbox
22. Click the "3D view" command in the View menu
23. Use the mouse to zoom and rotate the model
24. Use Sequence to calculate a complete wing's polar
25. Click on the "Polars" command in the View menu, (  ) to visualize the polar graphs

#### 4.3.18 Non convergences

	Cause	Fix
All methods	The foils' Type 1 polar meshes do not cover the available flight envelope [most usual case of non convergence]	Extend the foils' Type 1 polar meshes
	In Type 2 analysis, the lift is negative	Calculate only for higher values of the angle of attack
	In Type 2 analysis, the speed is either too low or too high, leading to OpPoints outside of the available flight envelope	Extend the foils' Type 1 polar mesh ; The speed will tend towards infinite values at low aoa, and symmetrically will tend towards 0 at high aoa
	The tip chord is too small and yields too low Reynolds numbers	Either: <ol style="list-style-type: none"> <li>1. Check the "Store OpPoints outside the Polar mesh" checkbox</li> <li>2. Omit the end of the wing in the definition of its planform</li> </ol>
LLT	The relaxation factor is too small	Increase the factor in the "LLT Settings..." dialog box
	The number of points over the planform is too high	Decrease the number in the "LLT Settings..." dialog box
VLM	The matrix is singular because of a conflicting disposition of VLM panels	Regenerate a manual VLM mesh
Panel	The results are inconsistent because the wakes shedded by the wing and elevator are in the same horizontal plane	Offset either the wing or elevator in the z direction, so that they do not lie in the same plane

Table 3: Non convergences causes and solutions

The log file will indicate which points of the flight envelope could not be calculated. It can be accessed with the menu command "Operating Point/View Log File"

The "log file" is a plain text file. If the document does not show up when called from the menu, it may be necessary to manually associate the ".log" extension to Windows' Notepad.

---

## 4.4 Stability and control analysis

The intent of stability and control analysis is to evaluate the time response of a plane to perturbations from a steady flight condition. The perturbations can originate with the environment, for instance from a gust of wind, or from the actuation of a control.

The mathematical representation of the response is a complex matter, which requires some simplifying assumptions. Essentially, only small perturbations about the steady flight conditions are considered.

The theoretical aspects of flight dynamics and stability analysis can be found in reference [1]. The purpose of this document is:

- to provide a short and much simplified description of the flight dynamics for users not familiar with the theory
- to explain the choices made in XFLR5
- and to describe the analysis procedure.

Note : the mathematical concepts and formulas presented hereafter are not absolutely necessary to the understanding of the physics of flight dynamics. They are provided as information and background for those users interested in investigating further the concepts.

### 4.4.1 Method

### 4.4.2 Theory

XFLR5 follows the method proposed by Etkin in ref [1].

With this type of analysis, longitudinal and lateral dynamics are independent and are evaluated separately.

### 4.4.3 Frames of reference

Three different reference frames come into consideration in stability analysis : the geometric axes, the body axes and the stability axes. These are defined in Figure 43.

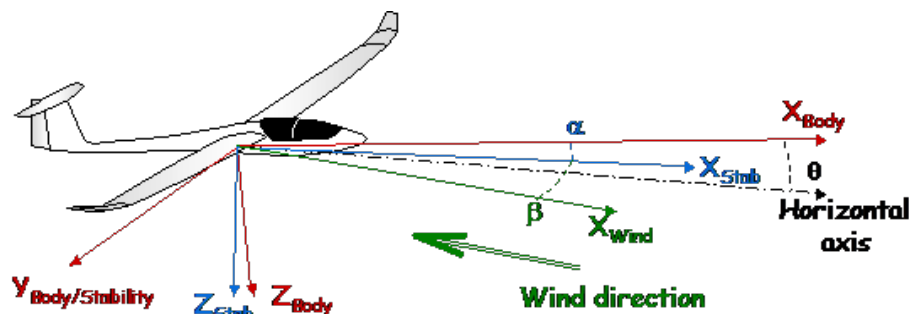


Figure 43: Body and stability axes

Body axes:

The term body axes is generic and refers to any frame which is fixed to the body, and is therefore not an inertial frame of reference. A usual, but not universal, convention is as follows:

- the  $X'$ -axis is aligned with the fuselage nose;
- the  $Z'$ -axis is in the plane of symmetry, and points downwards;
- the  $Y'$ -axis is perpendicular to the  $XZ$ -plane and points starboard.

#### Geometric axes:

This is the reference frame in which the geometry is defined.

- the  $X$ -axis is aligned "backwards"
- the  $Z$ -axis is in the plane of symmetry, and points upwards;
- the  $Y$ -axis is perpendicular to the  $xz$ -plane and points starboard.

The geometric axes are a special case of body axes.

#### Stability axes:

This is the frame in which the movement in the steady state conditions is most conveniently described:

- the  $x$ -axis is the projection of the velocity vector on the body's  $xz$ -plane; this axis therefore points forward
- the  $z$ -axis points downwards
- the  $y$ -axis points starboard

The point of origin of the frame is the plane's centre of gravity CoG.

The stability axes are a special case of body axes.

#### Notes:

- In horizontal level flight, the axis  $X_{stability}$  is horizontal
- Since sideslip in XFLR5 is simulated by rotation of the structure around the inertial  $Z_E$  axis, the wind axes are the same as the stability axes even if the sideslip is non zero.
- In equilibrium conditions, the stability axes are fixed to the body, and therefore are not an inertial frame.

XFLR5 follows the recommendation of [1] and performs all calculations in stability axes.

#### **4.4.4 Coordinates, position, velocity, and rotation vector**

The position of the body in stability axes is defined in some inertial frame of reference by the position of its origin  $O(x,y,z)$ , and by the rotation defined by Euler angles  $(\varphi, \theta, \psi)$ . Let  $V(U,V,W)$  be the body's velocity vector, and let  $\omega(P,Q,R)$  be the body's rotation vector, both defined in the stability axes.

Additionally, assume that the plane is in equilibrium flight, for instance :

- steady level flight with no sideslip
- banked circle turn



- 
- looping at constant speed (difficult to imagine, but no matter)

The state of the body/plane is defined by the set of variables (X, Y, Z, U, V, W, P, Q, R)

Since we shall be considering only small variations about the steady state conditions, each variable can be defined by an average value and a perturbation around this mean value. For instance:

$$U = U_0 + u$$

The subscript 0 refers to the steady flight state conditions.  $U_0$  for instance is the speed in level flight along the stability x-axis.

The purpose of stability analysis is to calculate the time response of the flight variables in response to small perturbations.

#### 4.4.5 Flight constraints

The stability derivatives are computed about equilibrium conditions. The conditions that are considered are level or banked horizontal flight. Using terminology from AVL :

$\alpha$  angle of attack

$\beta$  sideslip angle

$C_L$  Lift coefficient, calculated from the geometry,  $\alpha$  and  $\beta$ .

$\varphi$  arbitrary bank angle, positive to the right

**m** mass

**g** gravity acceleration

$\rho$  air density

**S** reference area

The constraints are :

- $U_0 = \sqrt{\frac{2mg}{\rho S C_L} \cos \varphi}$  airspeed
- $R_0 = \frac{V_0^2}{g} \tan \varphi$  turn radius, positive for right turn
- $W_0 = \frac{V_0}{R}$  turn rate, positive for right turn
- $p_0 = 0$  roll rate, zero for steady turn
- $q_0 = W_0 \sin \varphi$  pitch rate, positive nose upward
- $r_0 = W_0 \cos \varphi$  yaw rate, positive for right turn

Type 2 analysis in XFLR5 only considers the condition  $\varphi=0$ . This condition is relaxed for stability analysis.

#### 4.4.6 State description

The plane's state at any instant is given by a set of 8 variables. Four variables describe the longitudinal state:

**u** is the variation of speed along the x-axis :  $U = U_0 + u$

**w** is the variation of speed along the z-axis

**q** is the pitch rate, i.e. the rotation vector around the y-axis

$\theta$  is the pitch angle, i.e. the angle between the stability x-axis and the horizontal flight line

the angle is positive for a nose up.

Four variables describe the lateral dynamics:

**v** is the variation of speed along the w-axis

**p** is the roll rate, i.e. the rotation vector around the x-axis

**r** is the yaw rate, i.e. the rotation vector around the z-axis

$\varphi$  is the bank angle, i.e. the angle between the stability y-axis and the horizontal flight line



the angle is positive for a right wing down

The position defined by (x,y,z) does not come into consideration when studying flight dynamics, since the behaviour is not expected to depend on absolute position. The variation of gravity and density with altitude is negligible for model aircraft and is not taken into account.

In lateral dynamics, the heading  $\psi$  does not appear in the equations.

#### 4.4.7 Analysis procedure

The stability analysis follows the following steps:

1. Define the geometry
2. Define the mass, center of gravity (CoG), and inertia of each component of the plane. Two sub-options
  - (a) Enter the mass of the wing or body, and let XFLR5 estimate the inertia and CoG
  - (b) Enter those values manually
3. Define a stability Analysis/Polar (  +  ).

If no active controls are defined, the analysis will be run for the base geometry.  
If controls are defined, then the stability data may be calculated in a sequence for a range of control parameter, and a polar curve may be generated
4. Run the analysis for some control parameter. The code will

- 
- (a) Search for an angle of attack such that  $C_m=0$ , and will exit with a warning if unsuccessful
  - (b) Calculate the trim speed to achieve steady state flight
  - (c) Evaluate the stability derivatives,
  - (d) Build the state matrices,
  - (e) Extract the eigenvalues, and will exit with a warning if unsuccessful,
  - (f) Store the data in an OpPoint (optional) and in the polar object.

5. Visualize the results.

#### 4.4.8 Input

**Description** In input, the analysis takes :

- the plane's geometry
- the plane's mass, CoG and inertia tensor, defined in geometrical body axes.
- the parameters defined by the stability analysis
- the position for the controls : wing and elevator tilt angles, flap positions, etc.
- the type of steady flight to be considered : steady level flight or steady banked turn.

**Inertia estimations** A calculation form is provided to evaluate approximately the CoG position and the inertia tensor associated to the geometry. The evaluation should not be understood as anything else than a rough order of magnitude (ROM).

The inertia of the plane sums up the inertia of each object and of the additional point masses.

**Object inertias** The inertia of each object, i.e. wing or body, is evaluated in the dialog form for this object. It includes the volume inertia from the structural masses, and the inertia of point masses.

The volume inertia is evaluated based on the mass provided, and on the geometrical data defining the object. It is evaluated in the geometrical coordinate system, with origin at each object's CoG.

The evaluation is based on the following assumptions.

- For the body, the mass is distributed uniformly in the external surface, and this surface is assumed to have a uniform thickness. The body is divided in  $N_b$  elementary sections along the x-axis. The weight is concentrated at the center of the cross section, as illustrated in Figure 44.
- For the wing, the mass is assumed to be distributed uniformly in the wing volume along the span.  
In XFLR5 v5, it has been modeled as point masses concentrated at the quarter-chord point of distributed sections along the span.  
In XFLR5 v6, it is modeled as point masses distributed both in the span and chord directions, as illustrated in Figure 45. The mass distribution is independent of the wing's mesh used for aerodynamic calculations.

**Point masses** Parts such as actuators, battery, nose lead, or receiver should be modelled separately as point masses, and not be included in the evaluation of the volume inertia.

**Total inertia** The total inertia for a plane is the sum of the inertias of the object making up the plane, and of point masses. It is expressed in the reference frame defined by the plane's CoG and by the geometrical axes.

The transport of the inertia tensor from object CoG to plane CoG is done by application of Huyghens/Steiner theorem.

## Notes

- The mass defined for wings and bodies is not the one used for Type 2 calculations. The mass for type 2 is defined by the Analysis/Polar setting.
- The distribution of point masses should be adjusted to obtain the targeted position of the CoG. Otherwise, because of the approximations made in the automatic evaluation of volume inertia, a strict transposition of the "real" position of masses may result in an incorrect position of the plane's CoG.

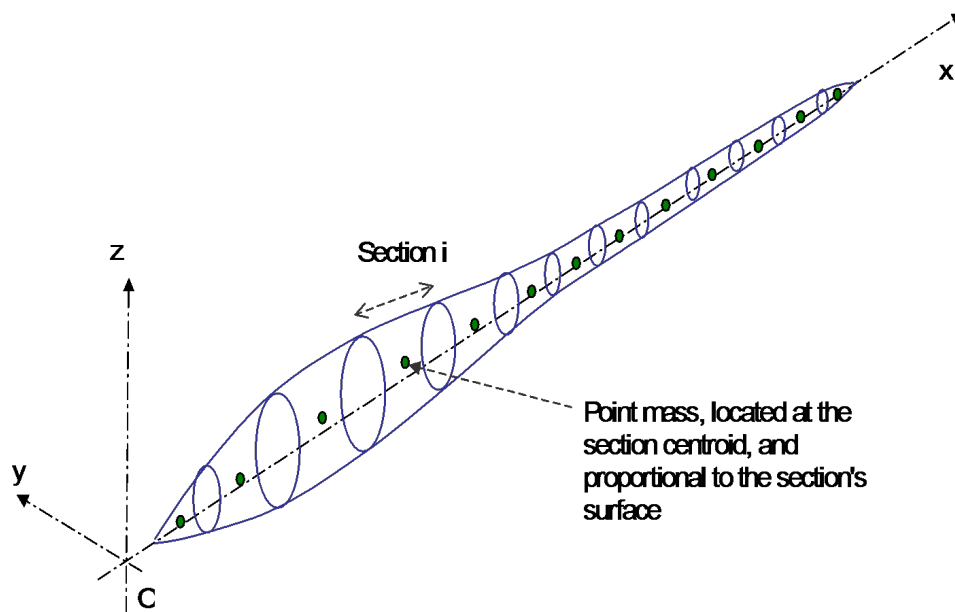


Figure 44: Mass representation for the body

**Stability polar parameters** The "stability polars" replace the former "control polars". The main difference is that the position of the CoG is no longer a variable, but is instead determined by the distribution of masses in the plane.

The Stability Polar object takes for input

- the fluid's density and dynamic viscosity
- the type of reference length and area for the calculation of aerodynamic parameters
- the selection of either viscous or inviscid analysis
- the control variables to include in the analysis

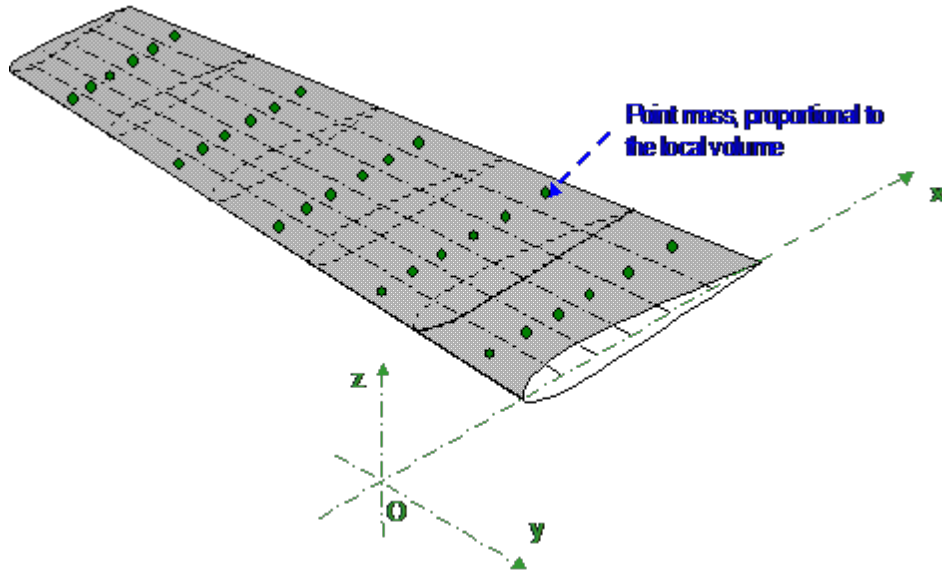


Figure 45: Mass representation for the wing

**Control variables** The polar points can be calculated for different state of control variables. These variables are:

- The tilting of the wing about the y-axis
- The tilting of the elevator about the y-axis
- the rotation of the main wing's flaps about their hinge axis
- the rotation of the elevator's flaps about their hinge axis
- the rotation of the fin/rudder's flaps about their hinge axis

Notes:

- The positive direction of rotation is positive by right-hand rule, i.e.
  - for the wing and elevator, a positive value will move the leading edge upwards and the trailing edge downwards
  - for a wing or elevator flap, a positive control value will move the trailing edge downwards
  - for the rudder, a positive control value will move the trailing edge to starboard
- To represent ailerons rotating in opposite directions, the min and max values of the controls for each wing's aileron should be opposite.
- The initial value of the control's angle is not taken into account in the analysis. For instance, if the flap has been defined with foils with non-zero flap angles, the initial angles will be cancelled before setting the position of the control. Similarly, the tilt angle defined for the wing or flap in the plane definition is cancelled before application of the control variable.

- For a control polar, all the parameters vary simultaneously in accordance with the value of the control parameter "c" :

$$Controlvariable = (1 - c) \times Control\_Min\_position + c \times Control\_Max\_position$$

- The rotation of controls is not represented in the 3D view

#### 4.4.9 Output

In output, the code provides results for longitudinal and lateral dynamics :

- The dimensional stability and control derivatives
- The non-dimensional stability derivatives
- the time response for a step input
- the eigenvalues and eigenvectors for the four longitudinal modes and the four lateral modes.

**Stability derivatives** The stability derivatives describe the change to a force or moment in response to a variation of a flight variable. For instance, the variation of the axial force resulting from a change in axial speed is:

$$\frac{\partial F_X}{\partial u} = \frac{1}{2}\rho \frac{\partial u_0^2}{S} C_X + \frac{1}{2}\rho u_0^2 S \frac{\partial C_X}{\partial u} = \rho u_0 S C_X + \frac{1}{2}\rho u_0^2 S \frac{\partial C_X}{\partial u}$$

A usual convention is to use simplified notations:

$$\frac{\partial F_X}{\partial u} = X_u$$

$$\frac{\partial C_X}{\partial u} = Cx_u$$

with both derivatives being calculated in the steady state.

$X_u$  is the dimensional stability derivative, and  $Cx_u$  is the non-dimensional stability derivative.

XFLR5 calculates the dimensional derivatives which are relevant at the scale of model sailplanes:

- In the longitudinal direction:  $(X_u, X_w, Z_u, Z_w, Z_q, M_u, M_w, M_q)$
- In the lateral direction:  $(Y_v, Y_p, Y_r, L_v, L_p, L_r, N_v, N_p, N_r)$

The non-dimensional derivatives are usually given in stability axes, and the derivatives w.r.t to v and w are provided instead w.r.t  $\alpha$  and  $\beta$ . They are :

- In the longitudinal direction  $CL_a, CL_q, Cm_a, Cm_q,$
- In the lateral direction :  $CY_b, CY_p, CY_r, Cl_b, Cl_p, Cl_r, Cn_b, Cn_p, Cn_r$

---

The definition of the non dimensional derivatives is :

$$CLa = Zw \times u0 / (q \times S)$$

$$CLq = Zq \times 2. \times u0 / (q \times S \times mac)$$

$$Cma = Mw \times u0 / (q \times S \times mac)$$

$$Cmq = Mq \times (2. \times u0 / mac) / (q \times S \times mac)$$

$$CYb = Yv \times u0 / (q \times S)$$

$$CYp = Yp \times 2. \times u0 / (q \times S \times b)$$

$$CYr = Yr \times 2. \times u0 / (q \times S \times b)$$

$$Clb = Lv \times u0 / (q \times S \times b)$$

$$Clp = Lp \times (2. \times u0 / b) / (q \times S \times b)$$

$$Clr = Lr \times (2. \times u0 / b) / (q \times S \times b)$$

$$Cnb = Nv \times u0 / (q \times S \times b)$$

$$Cnp = Np \times (2. \times u0 / b) / (q \times S \times b)$$

$$Cnr = Nr \times (2. \times u0 / b) / (q \times S \times b)$$

Where :

- q is the dynamic pressure,
- S is the reference Area
- b is the reference Span
- mac is the mean aerodynamic chord

The evaluation of the derivatives is an intermediate step in the calculation of the dynamic response. The derivative values are stored in the OpPoint object, and can be exported to a text file for use in other flight simulation codes.

**Modes** Natural modes

From the mathematical point of view, the state matrix can be diagonalized for eigenvalues and eigenvectors. An eigenvalue is of the form

$$\lambda = \sigma + i\omega$$

where

- $\sigma$  is the damping constant, unit 1/s
- $\omega$  is the circular natural frequency, unit rad/s

Any eigenvalue with a non-zero imaginary part  $\omega$ , has a symmetric eigenvalue given by the its conjugate. This implies that the time response of a variable for such a mode is of the form :

$$x(t) = Re^{\sigma t} \cos(\omega t - \phi)$$

where  $R$  and  $\phi$  are constant values determined by the initial conditions.

The mode will be dynamically stable if the damping is negative, unstable otherwise. Dynamic stability means that when disturbed, the plane will return progressively to its steady state flight.

Other definitions for oscillating modes :  $\omega_1 = \sqrt{\lambda\bar{\lambda}} = \sqrt{\sigma^2 + \omega^2}$  is the undamped natural circular frequency, unit rad/s.

For damped modes, i.e.  $\sigma < 0$ ,  $\zeta = \frac{-\sigma}{\omega_1}$  is the damping ratio, without unit :

- $\zeta > 1$  if the mode is overdamped
- $\zeta = 1$  if the mode is critically damped
- $\zeta < 1$  if the mode is underdamped, i.e. oscillatory

If the damping is weak, i.e.  $\zeta^2 < 1$ , then  $\omega_1 \approx \omega$ .

The frequency of vibration of the mode (unit Hz) is determined by :

$$F = \omega/2\pi$$

The time period (unit s) is :

$$T = 1/F = 2\pi/\omega$$

From the physics point of view, the eigenvalues and eigenvectors represent the natural modes on which the plane will tend to oscillate. For a standard well-defined problem, the modes will be:

- In the longitudinal case
  - two symmetric phugoid modes
  - two symmetric short-period modes
- In the lateral case
  - a roll damping mode



- 
- a spiral mode
  - two symmetric dutch roll modes

### Root Locus plot

The position of the eigenvalues may be represented in the complex plane, which is a convenient way to check visually the stability and frequency of the modes :

- Roots (eigenvalues) lying on the left of the diagram with negative x value correspond to stable modes, those lying on the right with positive x-value are unstable. The further down the left is the root, the more stable is the mode.
- Roots with non zero imaginary part correspond to oscillating modes, those with zero imaginary part are non-oscillating. The further away is the root from the x-axis, the higher is the frequency of vibration.

### Mode shape

The eigenvalue defines the mode's frequency and damping, and the eigenvector defines its shape.

It isn't an intuitive task to understand a mode shape from the eigenvector's components. Another more convenient way is to animate the mode in the 3D view.

Since the frequency and damping may be very different from one mode to the other, the time sampling and amplitude will need to be adjusted for each mode.

The mode amplitude R is arbitrary and has no physical significance. It may be adjusted to any scale for display purposes. In flight, a mode is seldom excited alone. Rather, an external perturbation will tend to generate a response on the different longitudinal and lateral modes. This can be modelled in the time response plot.

**Time response** The time response is evaluated based on the flight dynamics equation. For instance, in the longitudinal case, this is expressed as :

$$\begin{bmatrix} \dot{u} \\ \dot{w} \\ \dot{q} \\ \dot{\theta} \end{bmatrix} = [A_{long}] \cdot \begin{bmatrix} u \\ w \\ \theta \end{bmatrix} + [B_{long}] \cdot [F(t)]$$

where:

- $[A_{long}]$  is the 4x4 longitudinal state matrix,
- $[B_{long}]$  is the 4xn control influence matrix, with n being the number of control variables
- $[F(t)]$  is nx1 matrix, giving the forced input history of each control variable

Similarly for lateral modes:

$$\begin{bmatrix} \dot{v} \\ \dot{p} \\ \dot{r} \\ \dot{\varphi} \end{bmatrix} = [A_{lat}] \cdot \begin{bmatrix} v \\ p \\ r \\ \varphi \end{bmatrix} + [B_{lat}] \cdot [F(t)]$$

The time history of the state variables (u, w, q,  $\theta$ ) and (v, p, r,  $\varphi$ ) can be calculated either:

- as a consequence of perturbed initial conditions: this is the "Initial condition response"
- or as the consequence of control actuation vs. time : this is the "Forced response"

**Initial condition response** The input required is a step change from the steady state flight. For the longitudinal case, this input may be provided as any combination of values for  $u$ ,  $w$ , and  $q$ . In the lateral case, it is input as a combination of values of  $v$ ,  $p$ , and  $r$ .

**Open loop forced response** This type of analysis investigates the response of the plane to a change of a control parameter. Such parameters are typically a modification of thrust, or the actuation of a control surface such as the elevator, the rudder, or the ailerons. The modification of thrust is not considered in XFLR5.

The input required is a time history of a control parameter. XFLR5 only offers the possibility to simulate a linear ramp of a control in a finite time.

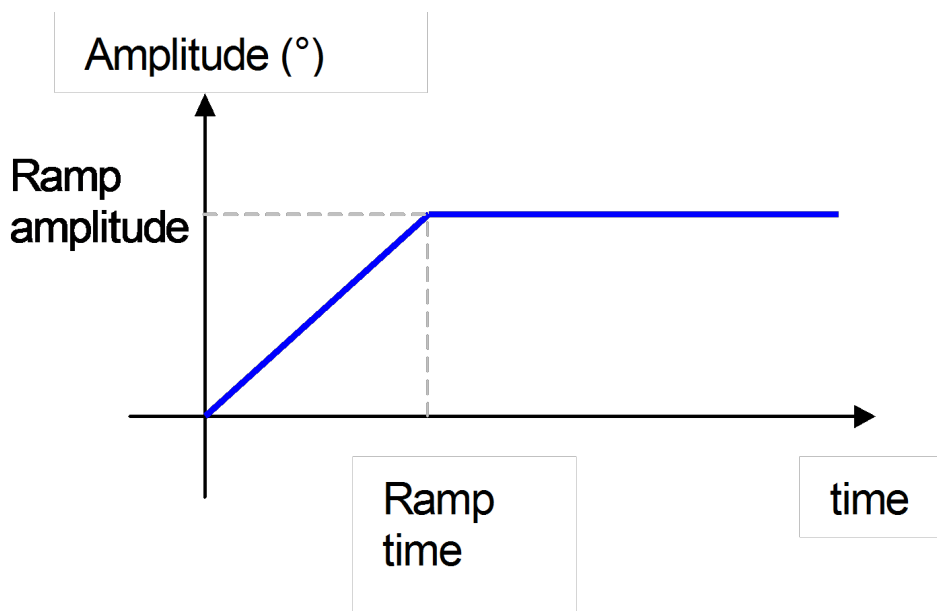








Figure 46:

Although all control variables are set simultaneously to determine the steady state geometry and trim conditions, the variation of each may be set independently in the evaluation of the forced response. The ramp time however is the same for all control variables.

Important note: the analysis of a response to a longitudinal step input may have physical relevance since the plane may eventually return to a steady state close to the initial conditions. On the opposite, the actuation of lateral control will lead to divergence from the steady state conditions, to coupling between longitudinal and lateral modes, and the analysis will not be representative. For instance, the ailerons will generate bank angle, modify the vertical lift, and will lead to divergence from the steady state conditions. The same goes for the actuation of the rudder, which will lead for instance to bank angle through dihedral effect.

#### 4.4.10 Session example – Stability analysis

Run steps 1 through 8 as in the wing analysis session described in §4.3.17.

- 
10. Optional, but recommended : Define the inertia properties of the current plane or wing object.
    - Select Current plane (or wing) / Define Inertia
    - Enter the inertia properties for the plane or wing.
    - Make sure that the CoG position is where it's meant to be. It may be necessary to "cheat" a little on the positions of point masses to achieve the desired position
    - Close the dialog box
  11. Optional : Click the "Define Analysis/Polar" in the Wing Polar menu,
    - select a type 1 or type 2 polar
    - Select "Use plane inertia", if previously defined
    - run a sequential analysis from low to high angles of attack
    - plot the graph  $ICm = f(\alpha)$ , make sure that the slope is negative and that there is some a.o.a for which  $ICm = 0$
  12. Click the "Define Stability Analysis" in the Wing Polar menu, or type  + 
  13. Either decide to use the previously defined object inertia, or input manually the mass, CoG position, and inertia properties
  14. Optional : activate a control, and decide on the range of variation
  15. Close the dialog box (  and  ). The polar's name should now appear in the top middle combobox.
  16. Select the control position in the right toolbar – start with 0. Deselect sequence.
  17. Check the "Store OpPoint" checkbox
  18. Click the "Analyze" button in the right toolbar
  19. If the analysis has been successful, an OpPoint is automatically added to the top right combobox. If not, check the log file to analyze the error message.
  20. In the polar view, check the "Show Point" checkbox for the polar. In the  $ICm = f(\alpha)$  plot, the point should be located precisely at the trimmed condition, i.e. at the angle of attack for which  $ICm = 0$
  21. Switch to the stability analysis  + 
  22. Select either the root locus plot, or the time response view or the 3D view

Carry on to define a stability analysis with activated controls, and view the stability properties as a function of control position.

## 5 Code Specifics

### 5.1 XFoil, AVL and XFLR5

XFLR5 has been developed based on XFoil V6.94. Later additions to XFoil have not been included in XFLR5.

Since the algorithms have been re-written and integrated in XFLR5, XFoil does not need to be present on the computer for XFLR5 to run. No special links need to be declared. XFLR5 does not use any of the AVL source code. The VLM algorithms have been developed and implemented independently.

For AVL files generated by XFLR5, the foil's file names will need to be checked, and it will also be necessary to check that the foil files are present in the directory together with the other AVL files.

### 5.2 Files and Registry

Running XFLR5 will generate two files in the user's directory for temporary files :

- "XFLR5.set" which records user settings ; delete this file to restore the default settings
- "XFLR5.log" which records the output of the foil and wing analysis


The location of the directory is defined by the user's environment variables.


XFLR5 itself does not write anything in the registry, but the installation program will create shortcuts for the ".plr" and ".wpa" files. Users can choose to associate the foil ".dat" files to XFLR5, but since this extension is used by Windows for many different purposes, it has been deemed preferable to leave this choice to the user.

Registry shortcuts will be removed by the uninstall process.


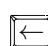
### 5.3 Shortcuts

In an attempt to increase the user friendliness of the interface, shortcuts have been provided for most major commands, and are mentioned in the menus.



Typing a first carriage return (  ) in a dialog box will select the OK or the default button, typing a second carriage return will activate this button.


Typing a first carriage return (  ) in the main window will select the 'Analyze' button, typing a second carriage return will activate this button.

### 5.4 Mouse input

All graphs, foils, and wings may be dragged and zoomed with the mouse. Using  +  button in 3D view will cause rotation of the model.

These options however may not work correctly (or not at all) if the buttons are not set to the "Default" in the Windows Mouse interface.

Pressing the  or  keys while zooming a graph will expand only the corresponding axis.

For those computers without a mouse wheel nor a middle button, zooming can be achieved in all views by pressing the  key and moving the mouse.

---

## 5.5 Memory

One of the characteristics of both the foil and the wing analysis is to use a significant computer memory.

Operating points specifically store a large amount of data and lead to voluminous project files which will slow down Save & Load processes. It is however unnecessary to keep them, since the important data is also stored in the polar objects which do not require large memory resources.

## 5.6 Export Options

### Printing

Although XFLR5, as it is, offers some printing options, the implementation of more advanced capabilities would require significant work, and has not been, nor is expected to become, the primary concern of the on-going development.

### Screen Images

An option has been added in v4.12 to export screen client areas to image files.

### Graph data

An option has been added in v4.13 to export graph data to text files.

### Data export

All results, operating points and polars, can be exported to text files for processing in a spreadsheet.

From v4.12 onwards, an option is available to export the data to the "comma separated value" format ".csv". This text format is meant to be readable without conversion in a spreadsheet. However, it may happen that the operating system's regional settings need to be adjusted to define the comma ',' as the default list separator.

## 5.7 Bugs

Once again, XFLR5 is by no means a professional program, and despite the author's best efforts and the help of all those who have tested it and provided valuable feedback, it is most probably still not default-free.

Main Bug Corrections :

1. In the 3D panel method implemented in XFLR5 v4, the formulation for Neumann boundary conditions was incorrect leading to inconsistent results. For this reason, the default method has used Dirichlet BC.  
The bug has been corrected in XFLR5 v6.02
2. A bug was reported shortly after the release of v3.00 on September 7<sup>th</sup>, 2006. It had for main consequence to count twice the elevator's lift in the calculation of a Plane with the VLM quad-method. This bug has been corrected in version v3.01 released on September 24<sup>th</sup>, 2006.
3. Up to v3.14, the contribution of the elevator and fin to the pitching and yawing moments was calculated with respect to the point X=0 instead of X=X<sub>CmRef</sub>.  
Corrected in v3.15 released January 21<sup>st</sup>, 2007.

The author will be grateful for any report of inconsistent results or other bugs, and will do his best to investigate and correct them in a timely manner. To facilitate bug corrections, the reports should ideally include:

- The Operating System's identification (e.g. Windows XP Pro, Vista...)
- The project file ("xxx.wpa")
- The sequence of commands leading to the bug

## 5.8 Open Source Development

On March 31<sup>st</sup>, 2007, XFLR5 has become an Open Source Development Project hosted by [SourceForge.net](https://sourceforge.net).

SourceForge provides a comprehensive set of tools and methods for a project's development, and a documentation may be found online. Potential contributors who would like to help organize the project, correct bugs, or add new features and enhancements are welcome.

## 6 Credits

Many thanks to Matthieu for his scientific advice and help, to Jean-Marc for his patient and comprehensive testing of the preliminary versions, to Marc for his natural ability to debug programs and planes, and to all the others who have contributed by their input to improve XFLR5, especially Giorgio and Jean-Luc.

Thanks also to Francesco who has written in RCSD 2008-04 a valuable tutorial for XFLR5, and who has contributed to the development of the version for MacOS

Similarly, thanks to Karoliina and Jean-Luc for her help in the compilation of the Debian/Ubuntu version.

Thanks also to Martin for the German translation, and to Jean-Luc for the French translation.

---

## 7 References

### References

- [1] James C. Sivells and Robert H. Neely, *Method for calculating wing characteristics by lifting line theory using nonlinear section lift data*. NACA Technical Note 1269, April 1947.
- [2] Robert H. Neely, Thomas V. Bollech, Gertrude C. Westrick, Robert R. Graham *Experimental and calculated characteristics of several NACA-44 series wings with aspect ratios of 8, 10 and 12 and taper ratios of 2.5 and 3.5*. NACA Technical Note 1270.
- [3] Katz & Plotkin, *Low Speed Aerodynamics, From wing theory to panel methods*. Cambridge University Press, 2<sup>nd</sup> Ed., 2001.
- [4] Brian Maskew, *Program VSAERO Theory Document*. NASA Contractor Report 4023, September 1987.
- [5] Sophia Werner, *Application of the Vortex Lattice Method to Yacht Sails*. Master Thesis, July 200.
- [6] André Deperrois, *About stability analysis using XFLR5* Presentation document, June 2008, [http://xflr5.sourceforge.net/docs/XFLR5\\_and\\_Stability\\_analysis.pdf](http://xflr5.sourceforge.net/docs/XFLR5_and_Stability_analysis.pdf).
- [7] André Deperrois, *Quelques notions d'aérodynamique de base et leur calcul dans XFLR5* Presentation document, June 2008, [http://xflr5.sourceforge.net/docs/Survol\\_Bases\\_Aero\\_et\\_XFLR5.pdf](http://xflr5.sourceforge.net/docs/Survol_Bases_Aero_et_XFLR5.pdf).
- [8] André Deperrois, *Illustration of the use of Control Polars in XFLR5* Presentation document, July 2008, [http://xflr5.sourceforge.net/docs/Control\\_analysis.pdf](http://xflr5.sourceforge.net/docs/Control_analysis.pdf).
- [9] André Deperrois, *Results vs. prediction* Presentation document, July 2008, [http://xflr5.sourceforge.net/docs/Results\\_vs\\_Prediction.pdf](http://xflr5.sourceforge.net/docs/Results_vs_Prediction.pdf).
- [10] Mark Drela & Harold Youngren, *Athena Vortex Lattice (AVL)*. <http://web.mit.edu/drela/Public/web/avl/>
- [11] B. Etkin and L.D. Reid *Dynamics of Flight: Stability and Control*. John Wiley and Sons, New York, NY, Third Edition, 1996.
- [12] André Deperrois, *Stability and Control analysis in XFLR5 v6*. Presentation document, September 2010, [http://xflr5.sourceforge.net/docs/XFLR5\\_and\\_Stability\\_analysis.pdf](http://xflr5.sourceforge.net/docs/XFLR5_and_Stability_analysis.pdf).